

Article

New Screening Protocol for Effective Green Solvents Selection of Benzamide, Salicylamide and Ethenzamide

Maciej Przybyłek *, Anna Miernicka, Mateusz Nowak and Piotr Cysewski *

Department of Physical Chemistry, Pharmacy Faculty, Collegium Medicum of Bydgoszcz, Nicolaus Copernicus University in Toruń, Kurpińskiego 5, 85-950 Bydgoszcz, Poland; 282892@stud.umk.pl (A.M.); 294597@stud.umk.pl (M.N.)

* Correspondence: m.przybylek@cm.umk.pl (M.P.); piotr.cysewski@cm.umk.pl (P.C.)

Abstract: New protocol for screening efficient and environmentally friendly solvents was proposed and experimentally verified. The guidance for solvent selection comes from computed solubility via COSMO-RS approach. Furthermore, solute-solvent affinities computed using advanced quantum chemistry level were used as a rationale for observed solvents ranking. The screening protocol pointed out that 4-formylmorpholine (4FM) is an attractive solubilizer compared to commonly used aprotic solvents such as DMSO and DMF. This was tested experimentally by measuring the solubility of the title compounds in aqueous binary mixtures in the temperature range between 298.15 K and 313.15 K. Additional measurements were also performed for aqueous binary mixtures of DMSO and DMF. It has been found that the solubility of studied aromatic amides is very high and quite similar in all three aprotic solvents. For most aqueous binary mixtures, a significant decrease in solubility with a decrease in the organic fraction is observed, indicating that all systems can be regarded as efficient solvent-anti-solvent pairs. In the case of salicylamide dissolved in aqueous-4FM binary mixtures, a strong synergistic effect has been found leading to the highest solubility for 0.6 mole fraction of 4-FM.

Keywords: solubility; green solvents; benzamide; salicylamide; ethenzamide; binary solvents; COSMO-RS; intermolecular interactions; affinity



Citation: Przybyłek, M.; Miernicka, A.; Nowak, M.; Cysewski, P. New Screening Protocol for Effective Green Solvents Selection of Benzamide, Salicylamide and Ethenzamide. *Molecules* **2022**, *27*, 3323. <https://doi.org/10.3390/molecules27103323>

Academic Editor: Jose C. Corchado

Received: 27 April 2022

Accepted: 20 May 2022

Published: 22 May 2022

Publisher's Note: MDPI stays neutral with regard to jurisdictional claims in published maps and institutional affiliations.



Copyright: © 2022 by the authors. Licensee MDPI, Basel, Switzerland. This article is an open access article distributed under the terms and conditions of the Creative Commons Attribution (CC BY) license (<https://creativecommons.org/licenses/by/4.0/>).

1. Introduction

Amides have been widely used in pharmacy as can be inferred from 649 records found in the DrugBank database [1–3]. Some examples are bacteria and antiviral agents (oseltamivir, cephalexin, ampicillin), anesthetics (lidocaine, bupivacaine, prilocaine), analgesics and nonsteroidal anti-inflammatory drugs (acetaminophen, salicylamide and ethenzamide). Some benzamide analogs for example salicylamide and ethenzamide are known for several decades and are used as over-the-counter medications in cases of headaches, migraine, cold and fever [4–6]. Technically speaking these active pharmaceutical ingredients (API) are ortho-substituted analogs of Benzamide and share several common features. All have moderate hydrophilicity ($\log P < 3$) and relatively low solubility in water, alcohols and other dissolution media. However, their weak dissolution abilities can be overcome through cocrystallization [7,8]. Importantly, the studies on the solid-state complexes showed that amides can interact very efficiently with aliphatic and aromatic carboxylic acids [7–12]. The basic properties of amides are associated with the resonance effect contributing to the electron density increase on the carbonyl oxygen atom [13,14]. Nevertheless, due to this effect, the N–H bond is more polarized, which implies proton-donating abilities enhancement. Hence, amides can form relatively strong intermolecular hydrogen bonds with proton-accepting compounds such as DMSO [15–18], DMF [18], acetone, tetrahydrofuran (THF) [19], acetonitrile [18,20] and 1,4-dioxane [18].

Solubility is one of the basic properties characterizing pharmaceuticals. This can be explained by the relationships between solubility and bioavailability, which have been

extensively studied [21–24]. Nevertheless, there are various technical issues closely associated with drug manufacturing, which cannot be underestimated. Indeed, solvents are used in every important step of drug development including synthesis, crystallization, extraction, and final form development. According to the Pharmaceutical Roundtable of American Chemical Society's Green Chemistry Institute (ACSGCI), organic solvents comprise an average of 54% of chemicals and materials used in the technological processes of the pharmaceutical industry, and hence the recycling, waste reduction, azeotropy (energy costs reduction during evaporation) and solvent safety are issues of particular importance in the context of sustainable pharmaceuticals' production design [25]. The high solubilizing ability, which enables the dissolution of a wide range of organic compounds, is also an important feature that distinguishes green solvents, especially when considering extraction processes. [26,27]. For this reason, it is crucial to develop strategies for selecting solvents that meet efficiency, safety, environmental hazard, and human health protection requirements. In recent years there has been growing interest in exploring solubility and partitioning properties of various compounds. A special attention should be paid for pharmaceuticals and nutraceuticals in green solvents such as ionic liquids [28–32], bio-based solvents including natural deep eutectic solvents (NADES) [33–39] and some environmentally friendly synthetic organic solvents, such as ethanol or DMSO and their organic-organic and organic-aqueous mixtures [40–43]. The application of multicomponent solvents containing water are interesting because it is possible to replace the environmentally hazardous pure organic solvent with less harmful aqueous mixtures. Noteworthy, although water is often considered an anti-solvent compared to organic solvents, in some cases, it can enhance the solubility, as a result of a significant co-solvation effect. Such synergism was frequently observed in many aqueous binary mixtures as for example for sulfamethizole in 1,4-dioxane [40,44] or acetonitrile binary mixtures [40], sulfanilamide in ethanol, acetonitrile and 1,4-dioxane [45,46], nicotinamide in DMSO and acetonitrile [18], phenacetin in 1,4-dioxane [47,48], amoxicillin in DMF-water [49] and theophylline in aqueous DMF, DMSO, 1,4-dioxane, 1-propanol and 1-butanol [33,50,51].

It is worth emphasizing that due to a large number of neat and binary aqueous solvents potentially interesting from the pharmaceutical practice, it is difficult to find the most optimal ones using time-consuming experimental methods. Hence, theoretical screening enabling the rational selection of the most promising candidates seems indispensable. Unfortunately, despite great efforts [18,33,40,45,52–60], there is no universal and reliable way of predicting solubility in binary aqueous solutions from the molecular structure. Methods developed for proper back-computations of measured solubility data such as Jouyban-Acree, van't Hoff-Yaws, Wilson, Apelblat, Buchowski-Ksiazczak and Non-Random Two Liquid (NRTL) are interesting from the thermodynamic interpretation viewpoint [45,61–64], however rather of limited applicability as screening tools. Hence, the first principle approaches seem to be attractive, even if prediction accuracies are only semi-quantitative or qualitative [55,65,66]. Among many of them the COSMO-RS methodology [67], is a very powerful tool applied for predicting various physicochemical properties using exclusively information of the chemical formula. In addition to many molecular affinity-related properties such as activity coefficients [68,69], equilibrium constants [70–72], cocrystals and solvates screening [10,11,67,73–77], phase diagrams [78–87], solubility in neat and multicomponent solvents [18,33,40,45,55,61,74,88–95], solubility parameters estimation [96–99] and partition coefficients [92,100–102] were computed with varying success. Nevertheless, this method is relatively efficient and allows determining the thermodynamic characteristics of mixtures based on the optimized 3D molecular structure. The use of molecular modeling methods facilitates directing experimental efforts to a limited population of systems, thereby allowing for saving time and chemicals. The latter aspect is of particular importance in the context of green and sustainable strategies.

The aim of this study is threefold. Firstly, the pool of experimental solubility data is extended by providing new results obtained for titled compounds in two proton accepting organic solvents (DMSO and DMF) and their aqueous mixtures. The choice of DMSO

and DMF was mainly guided by previous research showing their high efficiency in the case of other amides and sulfonamides [18,40,45,47]. Secondly, the accuracies of solubility computed using the COSMO-RS methodology were carefully checked against available experimental data of benzamide, salicylamide, and ethenzamide. Finally, the obtained model was used for finding efficient and environmentally friendly aqueous binary mixtures and new solubility measurements were performed for gaining information on solubility and external validation of the proposed screening protocol.

2. Results and Discussion

Solubility of the three selected aromatic amides was already the subject of serious interest as compiled in Table 1. The provided list encompasses pure water and 20 neat organic solvents. Additionally, ethenzamide solubility was determined by Tong et al. [103] in the binary mixtures of acetonitrile with either methanol, ethanol, or isopropanol. This study also provides the solubility in neat components. The other two aromatic amides were not studied in any mixed solvents.

Table 1. List of neat solvents for which experimental solubility of studied aromatic amides were experimentally determined.

Neat Solvent	Benzamide	Salicylamide	Ethenzamide
water	[9]	[104]	
methanol	[9]	[104,105]	[103,106]
ethanol	[9]	[107]	[103,106]
1-propanol	[9]	[107]	[106]
isopropanol	[9]	[107]	[103,108]
1-butanol	[9]	[107]	[108]
2-butanol		[107]	[108]
isobutanol	[9]	[107]	[106]
2-methyl-2-Propanol		[107]	
1-pentanol		[107]	[108]
3-methyl-1-butanol		[107]	
1-hexanol		[107]	
1-heptanol		[107]	
1-octanol		[107]	
2-ethyl-1-hexanol		[107]	
1-decanol		[107]	
methyl acetate	[9]	[107]	[108]
ethyl acetate	[9]	[104,105]	[106]
ethyl formate			[108]
propyl acetate		[107]	[108]
butyl acetate	[9]	[107]	[108]
acetonitrile	[9]	[104,105]	[103,106]
DMF			[108]
tetrahydrofuran		[107]	
acetic acid		[104]	
acetone	[9]	[105]	[108]
1,4-dioxane		[107]	[108]
2-butanone			[108]
m-xylene	[109]		
dibutyl ether		[107]	

The equilibrium in the solid-liquid saturated systems is governed not only by the properties of solvents but also by the solid state including polymorphic or pseudopolymorphic transformations as well as solvates formation. Hence, the precise description of the solids is an important aspect of solubility determination. For this reason, the sediments collected after the shake-flask experiments for water and studied organic solvents were examined using differential scanning calorimetry (DSC) and Fourier transform infrared spectroscopy–attenuated total reflectance (FTIR-ATR) techniques. The detailed characteris-

tics of solid residues were provided in supplementary materials (see Figures S5–S10). In the case of solvate formation or polymorphic transformation, the absorption band shifts on the IR spectra are often related to new hydrogen bonding patterns. In the case of DSC thermograms, new phases can be detected by observing additional signals due to the heat transfer associated with polymorphic transition or pseudo-polymorph transformations. It happened that in all studied cases no physical change of the solids is observed since both IR spectra and DSC thermograms recorded for the sediments do not differ significantly from those recorded for pure reagent. Based on the available literature data and the measurements performed in this study, it can be concluded that benzamide, salicylamide, and ethenzamide do not show a tendency to undergo phase changes in aqueous and organic solutions. This conclusion is in good accord with already reported observation. According to Ouyang et al. (2019) benzamide solid form is not altered in contact with such solvents as water, methanol, ethanol, 1-propanol, isopropanol, 1-butanol, isobutanol, methyl acetate, ethyl acetate, butyl acetate, acetonitrile and acetone [9]. In the case of salicylamide, the only polymorphic transformation observed so far was with the use of high pressure [110]. According to studies on the solubility and crystal form of salicylamide in water, methanol, ethyl acetate, acetonitrile, acetone, and acetic acid [104,105], no solid phase polymorphic or pseudo-polymorphic transitions were observed. As reported by Wang et al. (2021) [108] no polymorphic transitions of ethenzamide were observed in all studied sediments coming from saturated solutions in isopropanol, 1-butanol, 2-butanol, 1-pentanol, methyl acetate, ethyl formate, propyl acetate, butyl acetate, DMF, acetone, 1,4-dioxane and 2-butanone). The same observation was also reported for ethenzamide in methanol, ethanol, 1-propanol, isobutanol, ethyl acetate, and acetonitrile [103,106].

2.1. Benzamide

As enumerated in Table 1 the solubility of benzamide was experimentally determined in 13 solvents in a broad range of temperatures. So far the highest solubility at ambient conditions was reported for neat methanol ($x_B = 0.092$) [9] and the lowest for water ($x_B = 0.002$) [9] and at elevated temperatures solubility typically slightly increases. It is rather quite expected that this modest solubility can be optimized using other not studied so far solvents. In many cases, the qualitative criteria of alternative solvents selection can be proposed based on chemical intuition. Indeed, the amide group can be considered as a proton-donating center active with proton-acceptor solvents. There are several popular solvents of this type commonly used for solubility measurements such as DMSO or DMF. Due to the absence of corresponding experimental data for benzamide, these two solvents were chosen as the first choice for further experimental investigations and to expand the pool of available solubility data. These two solvents are characterized by high efficiency in dissolving many solids, including active pharmaceutical ingredients [18,40,45,47,49,111,112]. Their solubilizing potential can be interpreted in terms of solute-solvent affinity and in the particular case of benzamide the expected structures and corresponding energetics, determined theoretically, are documented in Figure 1. According to the results of quantum chemistry computations quite high affinity of benzamide is expected for either of these two solvents. In addition, ketones and esters such as acetone or methyl acetate are expected to exhibit similar properties. However, benzamide affinity toward these aprotic solvents is significantly lower which is reflected by reduced solubility. On the other hand, interactions of benzamide with amphiprotic water and proton donating methanol are different. These two solvents form two-center hydrogen bonding with both parts of the amide group as exemplified in Figure 1. The value of ΔG_r for methanol is comparable to DMSO and DMF. Although, there is not any general straight relationship noticed between affinities and solubility it is interesting to notice that for a subclass of aprotic solvents there is a modest linear dependency with $R^2 \approx 0.9$. This fortunate circumstance supports DMF and DMSO selection as potentially good solvents for benzamide. Unfortunately, the former is definitely problematic from the environmental impact perspective. In general, DMF is considered a toxic compound causing hepatic disorders [113]. Although DMSO is much less hazardous,

and is by some studies considered a green solvent [114–116], there are reports on its side effects indicating the need for its replacement with greener alternatives [117,118]. It has been already documented [40] that morpholine analogs belonging to the same class of solvents as DMSO can be regarded as a real alternative to DMSO not only as an effective solubilizer but also from the perspective of environmental impact and costs of measurements. Indeed, previous studies documented that 4FM is a very promising solvent that meets the criteria of environmental friendliness and was found to be a greener alternative for DMF [40,119–124]. However, there is very little research on its solubilizing properties. A very few examples that can be found in the literature is solubility studies on methane, hydrogen sulfide, carbon dioxide [125], ethane [126], propane [127], and caffeine [55]. For this reason, it is worth exploring the solubility of benzamide and also other studied aromatic amides in 4FM and their mixtures with water. Additionally, the results of affinity computations support the selection of 4FM as a potential solubilizer of benzamide. The corresponding values provided in Figure 1 suggest both the same nature of solute-solvent interactions and high affinity as DMSO.

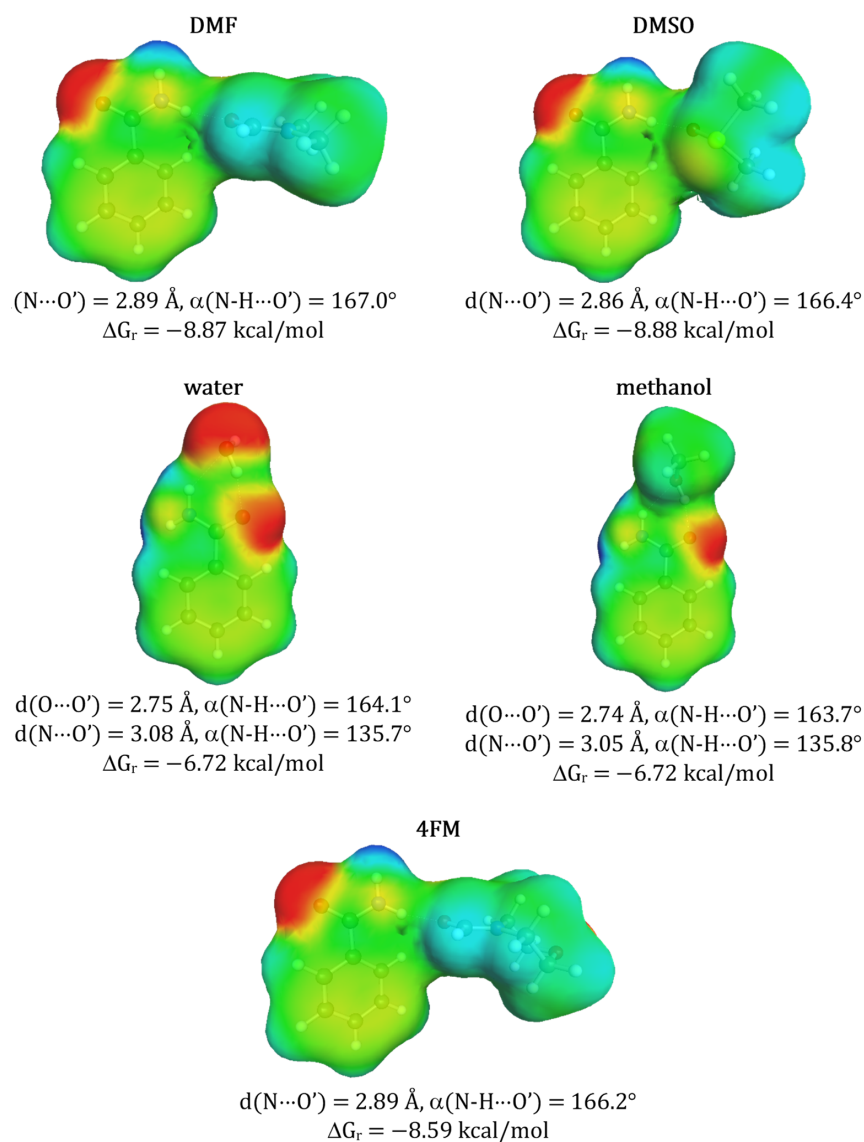


Figure 1. Structural and thermodynamic characteristics of selected solute-solvent contacts of benzamide. The affinity measure (ΔG_r) represents concentration-independent value associated with activity constant of the corresponding reaction of pair formation at room temperature. Prime denotes atoms belonging to solvent molecules.

However, before the actual selection of suggested aprotic solvents for benzamide solubility measurements additional and more qualitative screening has been performed based on the values of solubility computed using the COSMO-RS approach. The possibility of carrying out ab initio predictions directly from the molecular structure is very appealing [90]. Unfortunately, COSMO-RS formalism despite relying on chemical intuition, often fails in determining solubility [93,128–131] and other physicochemical properties [132–135]. Probably in most cases, the major explanation is the insufficient precision of available default parameterization [128,136], which on the other hand, in many cases provides quite an accurate match with measured values [56,90,91,137]. Fortunately, non-substituted benzamide is a relatively simple molecular system, which seems to be well-described by COSMO-RS. Indeed, the correlation between computed and experimental solubility (Figure 2) was found to be very satisfactory. Points marked with black ink represent the trend obtained for the set of already measured and published data. The data obtained for m-xylene were not included in the analysis since these old measurements correspond to much higher temperatures compared to other sets. The highly linear relationships between experimental and computed values enable extended screening of neat solvents not studied so far with the hope of finding better ones than already identified. Hopefully, this reduces the number of experiments to be performed. There are many potential green solvents which might be considered in such screening, since there are many various classification systems [123,138–144]. Here, the pool of solvents taken into account was adopted from the EPA (Environmental Protection Agency) [145] list provided by the solvent substitution Paris III software tool [146–150] suitable for evaluating the environmental impact of solvents. This protocol relies on the assessment of the overall environmental index (EI) including estimated parameters modeling the expected potential of human toxicity by ingestion (HTPIng), human toxicity by inhalation (HTPInh), terrestrial toxicity (TTP), aquatic toxicity (ATP), global warming (GWP), ozone depletion (ODP), photochemical oxidation (PCOP) and acid rain (AR). The initial set of 5423 solvents included in the Paris III program was shortened by imposing some practical restrictions. First of all, it is expected to find real and practical alternatives to commonly used solvents. Hence, those solvents which are not commercially available were excluded. This shortened the list to 3399 solvents. The second criterion was the environmental impact quantified based on indices proposed by EPA. The span of EI values ranged from 0.02 for water up to more than a million for chloranyl(methoxy)methane and chloranyl(chloromethoxy)methane. The latter compounds are considered very toxic. A very tight criterion was imposed on solvent “greenness” by including only such solvents, for which $EI < 2$. This resulted in 758 solvents, for which solubilities of benzamide were computed in 298.15 K. Noteworthy, such a tight criterion excluded the two initially selected solvents (DMSO and DMF). The computed solubility values assorted according to decreasing values of $\log(x_B^{est})$ were represented by gray crosses in the right part of Figure 2. All points placed above the gray dotted line indicate solvents assumed to be better than methanol and are supposed to be more efficient dissolving media for benzamide. It happened that the predicted benzamide solubility in DMSO is infinite, which is obviously incorrect. There are also other solvents for which the same outcome was computed as for example for 2-methoxyethanamine CAS = [109-85-3], diethylene glycol bis(3-aminopropyl) ether (CAS= [4246-51-9]) or tetren CAS = [112-57-2]. Despite the lack of actual solubility values, this prediction can be interpreted as an indication of the very high solubility of benzamide in these solvents. In addition, the solubility predicted in DMF is very high ($\log(x_B^{est}) = -0.60$). What is the most interesting the solubility of benzamide in 4FM seems to be also very high, $\log(x_B^{est}) = -0.61$. Hence, qualitative guidance based on chemical intuition, the nature of solute-solvent interactions and qualitative screening led to the same conclusion that 4FM might be a real alternative to other solvents. Taking advantage of this suggestion experimental work was carried out for Benzamide solubility determination in 4FM. Additionally, for comparison purposes, the solubility of benzamide was measured also in DMSO and DMF. Apart from the neat solvents, a series of aqueous binary mixtures were considered in four different ra-

tios of water and organic solvent. In Figure 3 the benzamide molar fraction solubility values corresponding to 298.15 K were presented. All measured solubility data are summarized in supplementary materials (Table S1). It is worth concluding that a systematic increase in solubility is observed with the increase of concentration of all solvents irrespectively of temperature. Moreover, the lack of synergistic effect and typical water antisolvent behavior shows that neat organic solvents are the best solubilizes. Their solubilizing power can be ordered as follows: DMF > DMSO > 4FM.

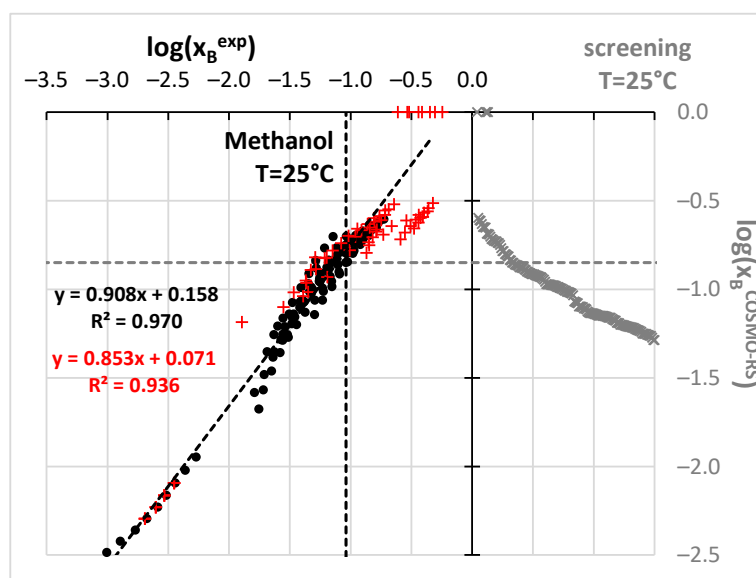


Figure 2. Results of benzamide solubility measurements and computations. All experimental points marked as black circles were taken from the literature while new measurements are presented as red pluses. Computed solubility values are presented in gray color. Dashed lines stand for best solubility values estimated so far at room temperature.

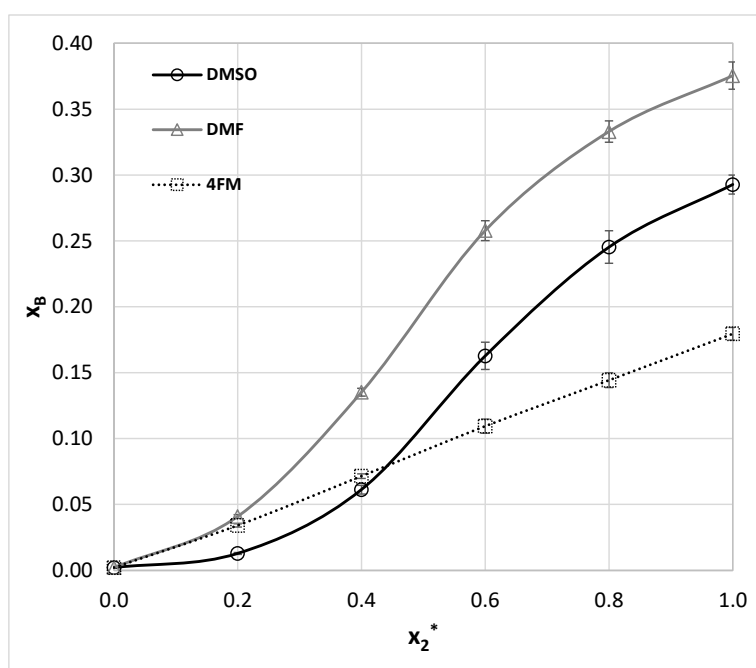


Figure 3. The results of benzamide solubility measurements (molar fraction, x_B) at room temperature in aqueous DMSO, DMF, and 4FM mixtures (x_2^* stands for the organic component mole fraction in the binary solvent). The error bars denote standard deviation values ($n = 3$).

To evaluate the green potential of experimentally studied water-organic solvents, the EI analysis was performed (Table 2). Each binary mixture was analyzed twice. Values corresponding to the default weighting of all contributions to EI were augmented with ones excluding of PCOP index in the analysis. This is justified by the fact that DMSO is commonly accepted as a green solvent but has a very high PCOP contribution. It is quite reasonable to ignore this parameter since PCOP is associated with the photochemical degradation in the atmosphere, which seems to be less important considering quite low volatility of DMSO and the absence of leaks in the technological equipment. Such simplification was already postulated [40,55]. Since, water is the most environmentally friendly solvent (EI = 0.02), with an increase in its proportion, the “green” potential of used solvents increases. Unfortunately, in most cases, solubility follows the opposite trend. If all the parameters are taken into account 4FM is the highest-ranked neat organic solvent. However, if the PCOP index is omitted then the DMSO-water mixture ($x_2 = 0.2$) is supposed to be the most environmentally friendly.

Table 2. The ranking of environmental friendliness of considered aqueous-organic solvents according to PARIS III tool [146–150]. The default impact factor, namely 5 was applied. The x_2 symbol denotes the organic component molar fraction in the binary mixture. In the parentheses, the values calculated without including the PCOP parameter were provided.

Solvent	X_2	HTPIng $\times 10$	HTPInh	TTP	ATP $\times 10^5$	GWP	ODP	PCOP	AR	EI	Rank
DMSO	0.2	0.73	0.00	0.07	3.23	0.0	0.0	5.94	0.0	6.09 (0.15)	12(2)
	0.4	0.99	0.00	0.10	4.61	0.0	0.0	8.49	0.0	8.69 (0.20)	13(3)
	0.6	1.14	0.00	0.11	5.38	0.0	0.0	9.90	0.0	10.10 (0.23)	14(4)
	0.8	1.24	0.00	0.12	5.87	0.0	0.0	10.80	0.0	11.00 (0.25)	15(5)
	1.0	1.30	0.00	0.13	6.20	0.0	0.0	11.40	0.0	11.70 (0.26)	16(6)
DMF	0.2	3.45	0.41	0.35	10.10	0.0	0.0	0.00	0.0	1.10 (1.10)	7(12)
	0.4	4.96	0.59	0.50	14.60	0.0	0.0	0.00	0.0	1.58 (1.58)	8(13)
	0.6	5.81	0.69	0.58	17.20	0.0	0.0	0.00	0.0	1.85 (1.85)	9(14)
	0.8	6.36	0.76	0.64	18.90	0.0	0.0	0.00	0.0	2.03 (2.03)	10(15)
	1.0	6.75	0.81	0.68	20.00	0.0	0.0	0.00	0.0	2.16 (2.16)	11(16)
4FM	0.2	1.60	0.00	0.16	61.40	0.0	0.0	0.00	0.0	0.32 (0.32)	2(7)
	0.4	2.07	0.00	0.21	80.90	0.0	0.0	0.00	0.0	0.42 (0.41)	3(8)
	0.6	2.31	0.00	0.23	90.50	0.0	0.0	0.00	0.0	0.46 (0.46)	4(9)
	0.8	2.44	0.00	0.24	96.10	0.0	0.0	0.00	0.0	0.49 (0.49)	5(10)
	1.0	2.54	0.00	0.25	99.90	0.0	0.0	0.00	0.0	0.51 (0.51)	6(11)

2.2. Salicylamide

Salicylamide was studied in a much-extended set of solvents compared to benzamide. Unfortunately for many systems only room temperature solubility was measured [107] and no data for aqueous-organic solvents mixtures are available. Hence, the pool of salicylamide

solubility data was extended by measurements in DMSO, DMF, and mixtures with water in the range of temperatures between 298.15 and 313.15 K. The obtained results are collected in supporting materials (see Table S2) and in Figure 4 for room temperature. According to available literature data, the best solvent for salicylamide found so far is THF, for which $x_S = 0.176$ [9]. As it was documented in Figure 4 both DMF and DMSO act as much more efficient solubilizers than THF and even significant dilution with water still leads to higher solubility potential.

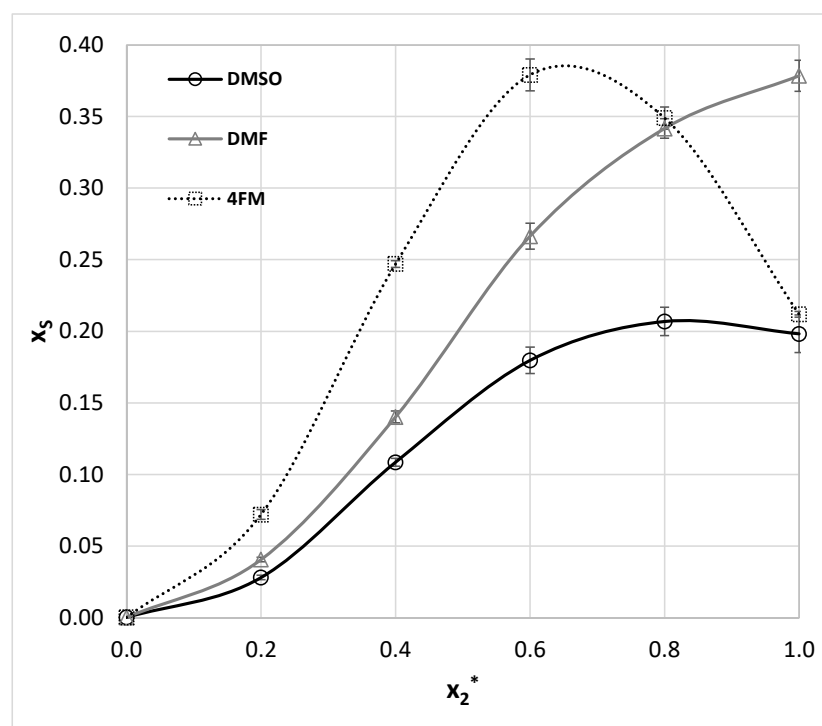


Figure 4. The results of salicylamide solubility measurements (molar fraction, x_S) at room temperature in aqueous DMSO, DMF, and 4FM mixtures (x_2^* stands for the organic component mole fraction in the binary solvent). The error bars denote standard deviation values ($n = 3$).

Although this finding is interesting on its own, it is worth following the same approach as applied to benzamide for screening of alternative solvents. In Figure 5 there is presented a relationship between computed and measured solubility values. The obtained correlation is quite satisfactory both for neat and binary solvents mixtures. However, despite the fact that the trend seems to be linear, there are many systems for which solubility is predicted with substantial inaccuracy. For example, solubility in acetic acid is seriously underestimated with a mole fraction error of magnitude -60% . In addition, salicylamide dissolution behavior in many solvents is misinterpreted as infinitely soluble. Among these problematic systems, one can find solvents with a high concentration of DMSO and DMF. On the contrary solubilities in alcohols are generally predicted by COSMO-RS with satisfactory accuracy. Nonetheless, the computed values are still informative and it is really interesting to point out that several solvents were identified as better compared to THF. It is not surprising that due to high structural similarities between salicylamide and benzamide 4FM was found as a potentially effective solvent. It is interesting to notice that a significant co-solvation effect occurs for the 4FM mole fraction of 0.6. This mixture is an effective solvent for salicylamide as neat DMF and the corresponding molar fraction solubility reached 0.379. Moreover, it is expected to be far more environmentally friendly ($EI = 0.46$) than pure DMF ($EI = 2.16$) (Table 2).

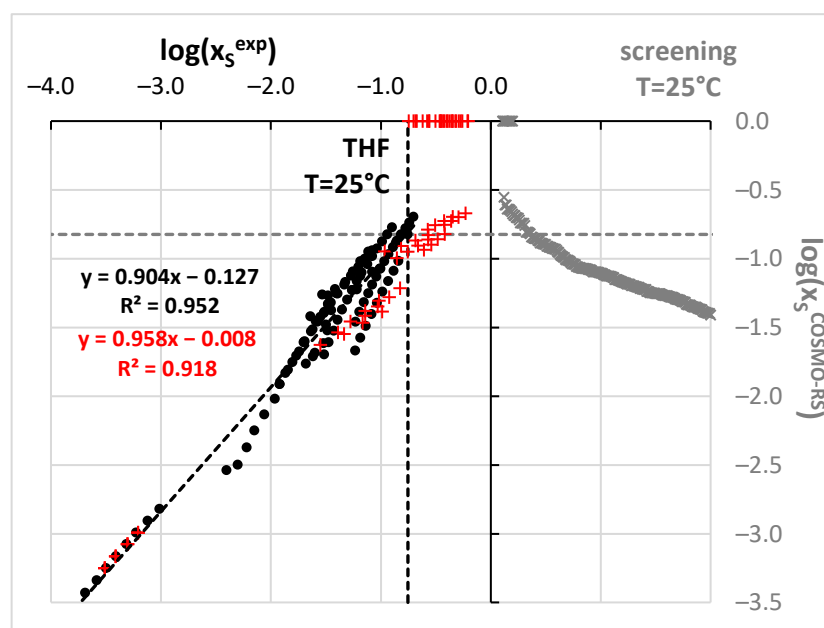


Figure 5. Results of salicylamide solubility measurements and computations. Notation is the same as in Figure 2.

Such high solubility of salicylamide in all three studied aprotic solvents can be explained by the solute-solvent affinities documented in Figure 6. The pairs formed between salicylamide and solvent molecule are stabilized by a strong hydrogen bond formed between the amide group acting as a donor and the electronegative center of the solvent molecule acting as acceptor. The affinity of salicylamide to DMSO was found to be the highest which nicely corresponds with observed solubility. Other aprotic and proton accepting solvents have similar affinities. The values of Gibbs free energy of hetero association are significantly smaller for water and methanol reflecting the significantly lower solubility of these solvents.

2.3. Ethenzamide

The solubility of this aromatic amide is available in 18 neat solvents as enumerated in Table 1. Additionally there were reported solubility values for three binary mixtures of acetonitrile with either methanol, ethanol or isopropanol [103]. Noteworthy, in all cases, the significant solubility enhancement through the co-solvation effect was observed, which shows the nontrivial solubilizing role of complex solvents containing both proton donating and accepting components. To extend the set of experimental data for ethenzamide three sets of aqueous binary mixtures were considered, by the analogy to measurements performed for other aromatic amides studied in this work. The obtained results were presented in a graphical way in Figure 7 for room temperature. The tabulated values can be found in supposing materials (Table S3). Considering published data the best solvent identified so far is DMF ($x_E = 0.063$ at 298.15 K). For consistency, ethenzamide solubility measurements in neat DMF were repeated and confronted with already published results by Wang et al. [108]. A comparison of these results with our data is provided in supporting materials (Figure S4) and it can be concluded that there is consistency between these two collections. As it is documented in Figure 7 all three aprotic solvents are very efficient solubilizers leading to the following sequence of the solubility: DMF > 4FM \approx DMSO. Noteworthy, when considering the organic-aqueous mixtures no synergistic effect occurs by adding water, which plays a typical antisolvent role.

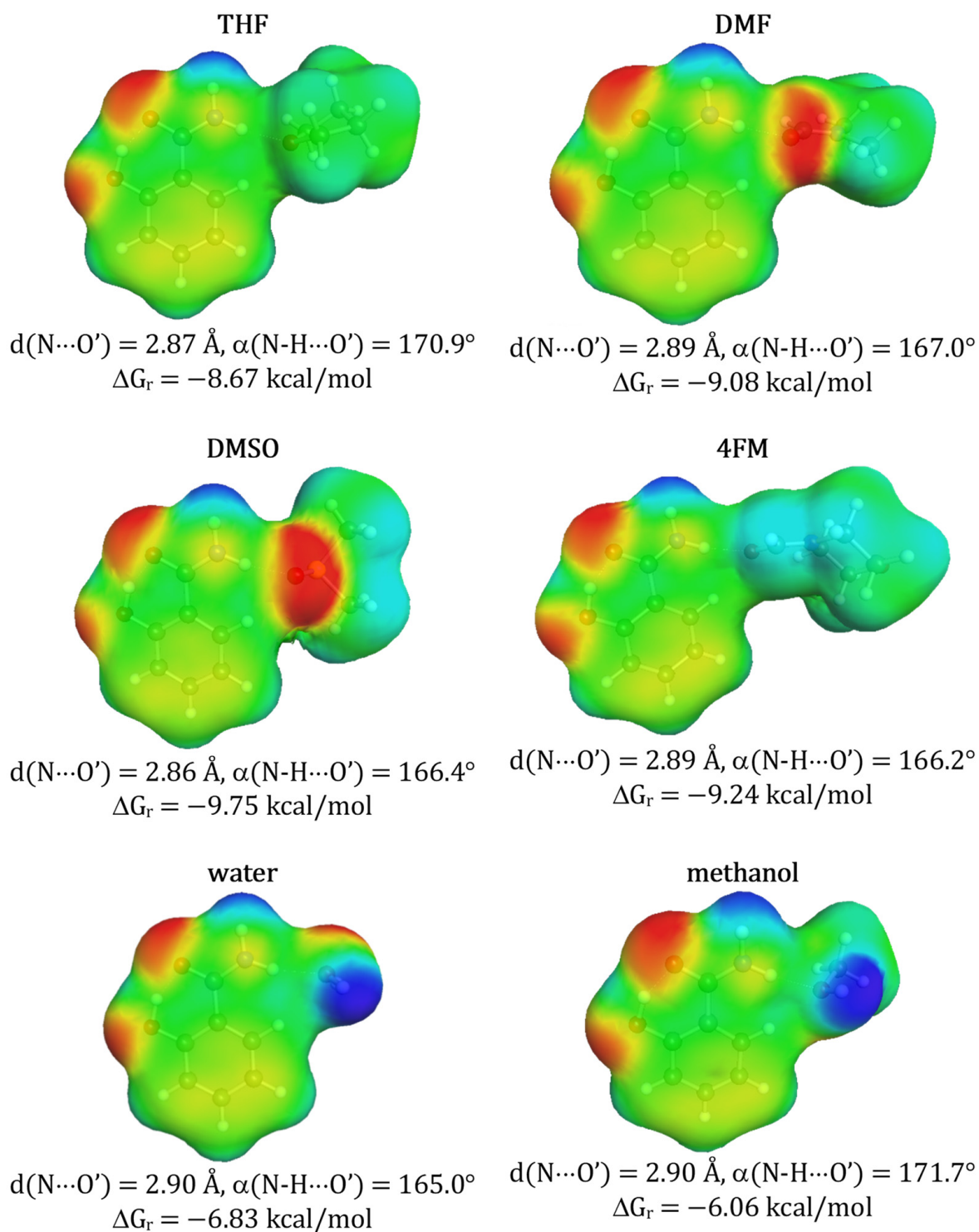


Figure 6. Structural and thermodynamic characteristics of selected solute-solvent contacts of salicylamide. Notation is the same as in Figure 1.

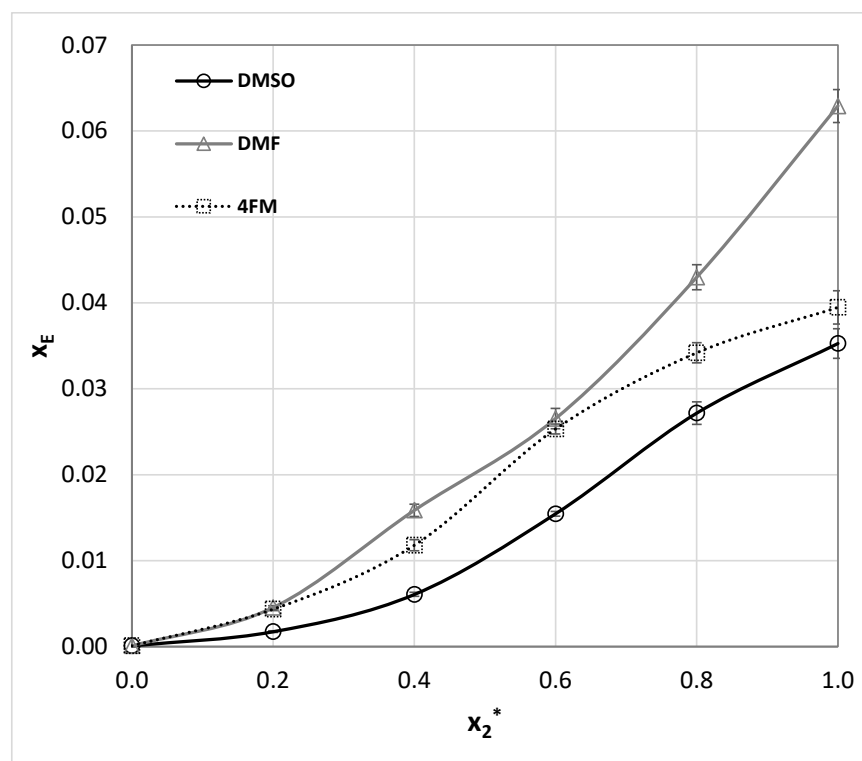


Figure 7. The results of ethenzamide solubility measurements (molar fraction, x_E) at room temperature in aqueous DMSO, DMF, and 4FM mixtures (x_2^* stands for the organic component mole fraction in the binary solvent). The error bars denote standard deviation values ($n = 3$).

Results presented in Figure 8 suggest that ethenzamide has a lower affinity to aprotic solvents and much higher to protic ones compared to Benzamide and Salicylamide. This might be related to the steric and electrostatic hindrance imposed by the presence of an ethoxy group at ortho-position and the formation of strong intramolecular hydrogen bond stabilizing ethenzamide which was already documented [10]. Consequently, the heteromolecular contacts of ethenzamide with aprotic solvent molecules have different structures than the ones observed for the other two aromatic amides. Furthermore, a very close distance between the oxygen atom of the ethoxy substituent and the amide group results in reducing the donating character of the hydrogen atom located on the latter. Consequently, all interactions with proton accepting molecules are significantly less favorable compared to benzamide and salicylamide. On the contrary, the oxygen atom of the amide group of ethenzamide acts as a stronger proton accepting center favoring hydrogen bonding with proton donating molecules, such as water and methanol. This is in accordance with the ΔG_r values obtained for protic solvents. However, in general, the affinities of ethenzamide to solvents molecules are significantly lower than in case of benzamide and salicylamide which is also associated with lower solubility.

To complete the analysis of ethenzamide solubility the COSMO-RS modeling was performed and the obtained results are collected in Figure 9. It is evident that the quality of theoretical prediction is much lower in this case. Difficulties in the prediction of ethenzamide solubility by using COSMO-RS were already noticed [93] and a more sophisticated approach is required for achieving adequate correspondence between computed and experimental data. Despite the poorer performance of the computational protocol compared to other aromatic amides, it is still possible to use the calculation results as qualitative guidance, and all aprotic solvents used for ethenzamide solubility measurements were properly identified.

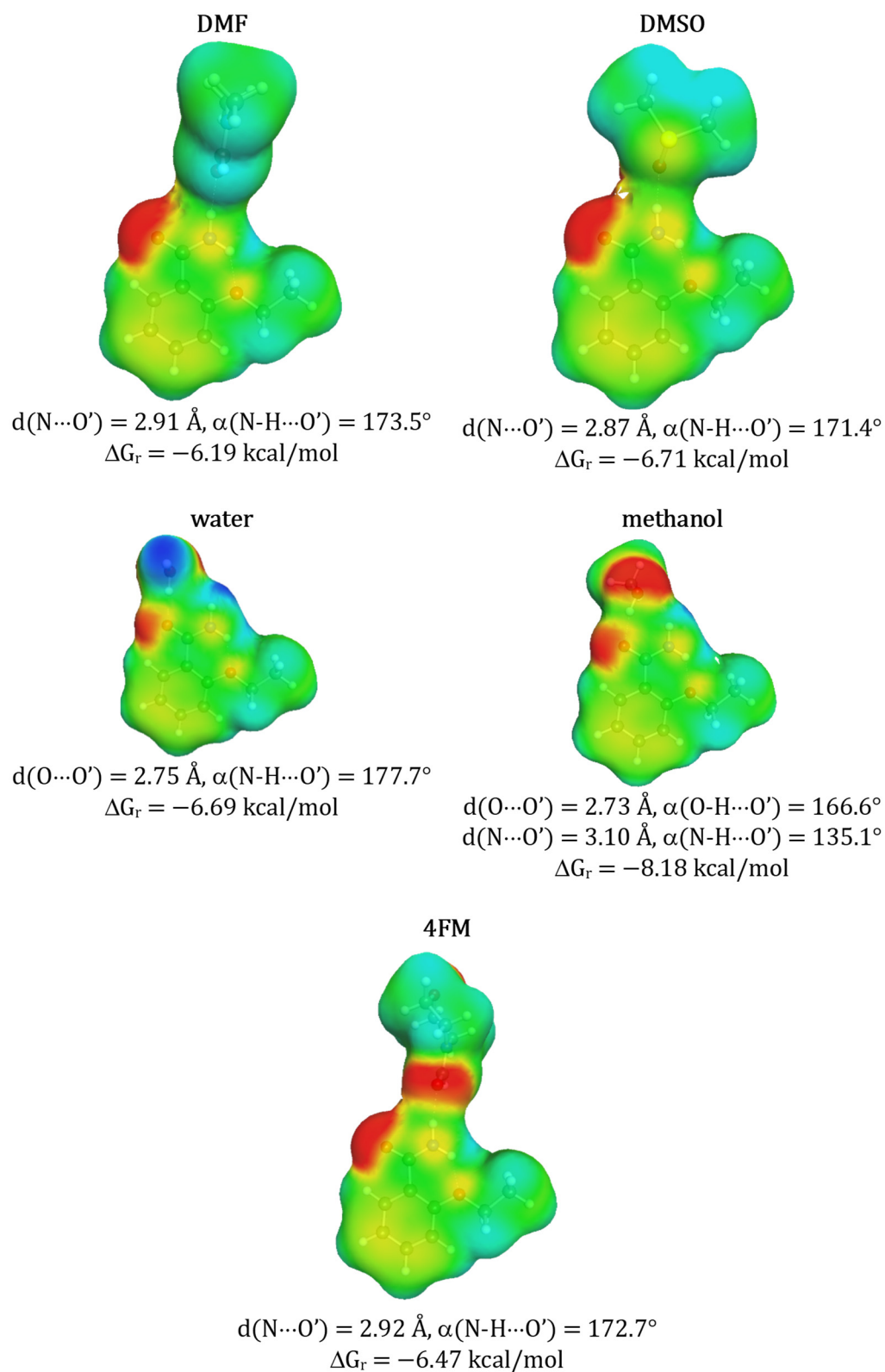


Figure 8. Structural and thermodynamic characteristics of selected solute solvent contacts of ethenzamide. Notation is the same as in Figure 1.

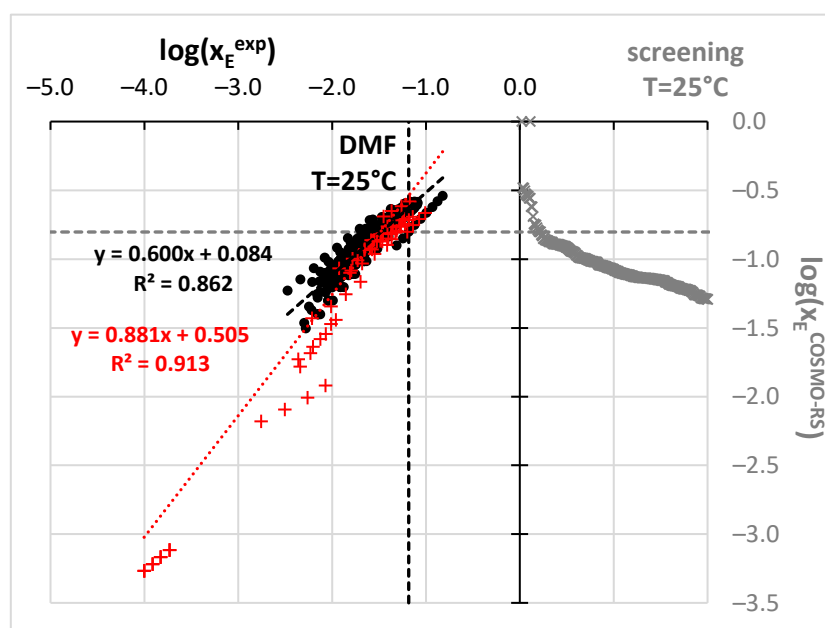


Figure 9. Results of ethenzamide solubility measurements and computations. Notation is the same as in Figure 2.

3. Materials and Methods

3.1. Chemicals

All chemicals applied in this study were purchased from commercial suppliers and used without purification. benzamide (CAS: 55-21-0, 99%), salicylamide (CAS: 65-45-2, 99%) and ethenzamide (CAS: 938-73-8, 97%) and 4-formylmorpholine (CAS: 4394-85-8, 99%) were purchased from Sigma-Aldrich (Poznań, Poland). dimethyl sulfoxide (CAS: 67-68-5, ≥ 99.7) and N,N-dimethylformamide (DMF, CAS: 68-12-2, $\geq 99.8\%$) were obtained from Avantor (Gliwice, Poland). Methanol (CAS: 67-56-1, $\geq 99.5\%$) was purchased from (Chempur, Piekary Slaskie, Poland). The nitrogen (99.999%) used for the DSC measurements was supplied by Linde (Warsaw, Poland).

3.2. Solubility Measurements Procedure

In this study, the “shake-flask” procedure used in the previous studies [18,33,40,45,47,55,61] was applied and it consists of the following steps. First, the mixtures (suspensions) containing saturated solution and undissolved solids were prepared in glass screw test tubes. Then the mixtures were incubated and agitated for 24 h at controlled temperature (298.15, 303.15, 308.15, or 313.15 K) and 60 rpm using Orbital Shaker ES-20/60 (Biosan, Riga, Latvia). At the next step, the temperature was still controlled, however, the agitation was turned off and suspensions were let to settle down for an hour. Then, the supernatant was filtrated using 0.22 μm PTFE syringe membrane filter. Next, 0.1 mL of the filtrate was diluted with 2 mL of methanol. The samples prepared in this way were protected against crystallization, as the concentration was low. 0.5 mL of the filtrate was used for density measurements. All equipment including automatic pipette tips, membrane filters, and syringes were preheated at the measurement temperature in order to avoid the solute precipitation. All “shake-flask” experiments were carried out in triplicate. The concentration in the samples was determined spectrophotometrically using the calibration curve method. The selected absorption maximum (λ_{max}) was 223, 302 and 290 nm for benzamide, salicylamide and ethenzamide, respectively. All UV spectra were recorded using an A360 UV-VIS spectrophotometer (AOE Instruments, Shanghai, China).

3.3. Solid Residues Analysis

The solid residues obtained after “shake-flask” procedure were dried on air and used for IR spectrophotometric and DSC measurements. Infrared spectra were recorded using PerkinElmer (Waltham, MA, USA) spectrophotometer equipped with a diamond attenuated total reflection (ATR) device. DSC thermograms were recorded using DSC 6000 Perkin Elmer (Waltham, MA, USA) calorimeter (heating rate: 5 K/min, nitrogen flow: 20 mL/min) calibrated using indium and zinc reference standards provided by the manufacturer.

3.4. Calculation Details

Theoretical characteristics of analyzed compounds started with conformational analysis for adequate representation of structural diversity. The initial structures were taken from the public PubChem database [151] and processed using the BIOVIA COSMOconf 2020 program [152] dedicated to generating the most energetically favorable conformations. The algorithm performs a series of optimizations and a number of structures reduction leading to the most probable conformers. The working part utilizes BIOVIA TURBOMOLE 2021 (release V7.5.1) [153] for geometry optimizations. The level of theory used at this stage corresponded to RI-DFT BP86 (B88-VWN-P86) with def-TZVP basis set for geometry optimization and def2-TZVPD basis set for single-point calculations with the inclusion of the fine grid tetrahedron cavity and inclusion of parameter sets with hydrogen bond interaction and van der Waals dispersion term based on the “D3” method of Grimme et al. [154]. The solubility calculations were performed using BIOVIA COSMOtherm 2021 [152] with BP_TZVPD_FINE_21.ctd parametrization. The protocol for solubility computations relies on iteratively solving the following equation,

$$\ln\left(\gamma_i^{sat,i+1} x_i^{sat,i+1}\right) = \frac{1}{RT} \left(\mu_i^{o,liq} - \mu_i^{(i)} \left(\gamma_i^{sat,i} x_i^{sat,i} \right) + \max\left(0, \Delta_{fus} \bar{G}_i^m\right) \right) \quad (1)$$

where superscripts i and $i + 1$ denote the values obtained in two subsequent iterations of solute chemical potential $\mu_i^{(i)} \left(a_i^{sat,i} \right)$, $a_i^{sat} = \gamma_i^{sat} x_i^{sat}$ defines activity, activity coefficients, and molar fraction solubility, $\mu_i^{o,liq}$ stands for solute chemical potential in the liquid phase and $\Delta_{fus} \bar{G}_i^m$ is the partial molar Gibbs energy of melting at the solubility measurements conditions. Since COSMO-RS theory was formulated for treating bulk phases the last value is to be provided as the additional input value. There is extended discussion [47,155–158] on how properly define this quantity. Here, the simplest approach was adopted by assuming that contribution coming from the values of capacity change upon melting is small and negligible. Hence, only melting temperature and heat of fusion are necessary for estimation of the values of Gibbs free energy of fusion. These values were taken from literature as averaged values of compiled by Acree et al. [159], namely for benzamide $T_m = 401.0$ K, $H_{fus} = 20.9$ kcal/mol, for salicylamide $T_m = 412.3$ K, $H_{fus} = 28.4$ kcal/mol, and for ethenzamide $T_m = 405.0$ K, $H_{fus} = 20.4$ kcal/mol.

Apart from solubility, the values of solute-solvent affinities were estimated similarly as in our previous studies [33,40,55] and here only brief remarks are provided. The affinity represents the values of Gibbs free energies of hetero-association reaction $X + Y = XY$, where X and Y stand either for solute or solvent molecules. The extended conformational analysis precedes the actual thermodynamic computations. Many potential bimolecular clusters were considered by taking into account molecular surface segments statistics invoked in COSMOtherm program via command “CONTACT = {1 2} ssc_probability ssc_weak ssc_ang = 15.0”. These structures were further underwent geometry optimization and clustering on the same level as monomers. Finally, the values of the equilibrium constant were computed with the inclusion of energies correction accounting for zero-point vibrational energy (RI-DFT BP86 (B88-VWN-P86)/def2-TZVPD level) and electron correlation (RI-MP2/def2-QZVPP level). The solute-solvent affinity was represented by concentration-independent activity-based values of the Gibbs free energy.

4. Conclusions

Pharmaceutically active compounds are very often examined in terms of their solubility in various one- and multi-component solvents. In this study the COSMO-RS solubility predictions of benzamide, salicylamide, and ethenzamide were combined with green solvents selection strategy. As was established, the landscape of environmentally friendly solvents characterized by the highest solubilization abilities comprises aprotic solvents. This fact is supported by much higher stability of the interactions formed with the amide group acting as a hydrogen bond donor than when it plays an acceptor role.

Despite certain limitations of the COSMO-RS model, which was of significant importance in the case of ethenzamide, the proposed approach of selecting green solvents characterized by high solubilizing abilities seems to be reasonable. However, further research on other classes of compounds is needed. Noteworthy, 4FM, which is considered green alternative for DMF was found to be a quite efficient solvent, especially for salicylamide and ethenzamide. Moreover, in the case of the former amide, a significant co-solvation effect was observed for the aqueous binary solvent ($x_s = 0.6$), which is also expected to be more environmentally friendly than pure DMF. This is a good example of how beneficial the co-solvation effect is in terms of selecting environmentally friendly substitutes for toxic solvents. Therefore, the use of molecular modeling to select the most effective green solvents from the list including the criteria proposed by EPA, and extending the research to experimental measurements of solubility in aqueous-organic mixtures is a useful and reliable strategy.

Supplementary Materials: The following supporting information can be downloaded at: <https://www.mdpi.com/article/10.3390/molecules27103323/s1>, Figure S1: The comparison of benzamide solubility profiles in binary solvents containing DMSO (a), DMF (b), 4FM (c). The organic component mole fraction in the binary solvent was denoted by x_2^* ; Table S1: Values of benzamide molar fraction solubility (x_B) in binary aqueous-organic solvents. x_2^* stands for the organic component mole fraction in the binary solvent; Figure S2: The comparison of salicylamide solubility profiles in binary solvents containing DMSO (a), DMF (b), 4FM (c). The organic component mole fraction in the binary solvent was denoted by x_2^* ; Table S2: Values of salicylamide molar fraction solubility (x_S) in binary aqueous-organic solvents. x_2^* stands for the organic component mole fraction in the binary solvent; Figure S3: The comparison of ethenzamide solubility profiles in binary solvents containing DMSO (a), DMF (b), 4FM (c). The organic component mole fraction in the binary solvent was denoted by x_2^* ; Table S3: Values of ethenzamide molar fraction solubility (x_E) in binary aqueous-organic solvents. x_2^* stands for the organic component mole fraction in the binary solvent; Figure S4: The comparison of ethenzamide solubility data in DMF obtained in this study and reported in the literature (Wang et al., J. Chem. Eng. Data 2021, 66, 1508–1514); Figure S5: The FTIR-ATR spectra recorded for the benzamide sediments collected after shake-flask experiments; Figure S6: The FTIR-ATR spectra recorded for the salicylamide sediments collected after shake-flask experiments; Figure S7: The FTIR-ATR spectra recorded for the ethenzamide sediments collected after shake-flask experiments; Figure S8: The DSC thermograms recorded for the benzamide sediments collected after shake-flask experiments; Figure S9: The DSC thermograms recorded for the salicylamide sediments collected after shake-flask experiments; Figure S10: The DSC thermograms recorded for the ethenzamide sediments collected after shake-flask experiments.

Author Contributions: Conceptualization, P.C.; methodology, P.C. and M.P.; validation, P.C. and M.P.; formal analysis, P.C. and M.P.; investigation, P.C., M.P., A.M. and M.N.; resources, P.C., M.P., A.M. and M.N.; data curation, P.C. and M.P.; writing—original draft preparation, P.C. and M.P.; writing—review and editing, P.C. and M.P.; visualization, P.C. and M.P.; supervision, P.C.; project administration, P.C. and M.P. All authors have read and agreed to the published version of the manuscript.

Funding: This research received no external funding.

Institutional Review Board Statement: Not applicable.

Informed Consent Statement: Not applicable.

Data Availability Statement: All available data were provided in the manuscript and Supplementary Materials.

Conflicts of Interest: The authors declare no conflict of interest.

References

1. Janardhan, S.; Ram Vivek, M.; Narahari Sastry, G. Modeling the permeability of drug-like molecules through the cell wall of: Mycobacterium tuberculosis: An analogue based approach. *Mol. Biosyst.* **2016**, *12*, 3377–3384. [CrossRef] [PubMed]
2. DrugBank. Available online: <https://go.drugbank.com/> (accessed on 25 April 2022).
3. Wishart, D.S.; Knox, C.; Guo, A.C.; Shrivastava, S.; Hassanali, M.; Stothard, P.; Chang, Z.; Woolsey, J. DrugBank: A comprehensive resource for in silico drug discovery and exploration. *Nucl. Acids Res.* **2006**, *34*, D668–D672. [CrossRef] [PubMed]
4. Wang, P.J.; Guo, H.R. Frequent analgesics consumption in migraineurs: Comparison between chronic and episodic migraineurs. *J. Headache Pain* **2004**, *5*, 30–35. [CrossRef]
5. Huang, B.C.; Lien, M.H.; Wang, P.Y.; Chang, B.L. Interference by drugs contained in over-the-counter cold syrups on methamphetamine immunoassay test kits used in drug abuse assessment. *J. Food Drug Anal.* **1995**, *3*, 259–268. [CrossRef]
6. Batterman, R.C.; Grossman, A.J. Effectiveness of salicylamide as an analgesic and antirheumatic agent: Evaluation of the double blindfold technique for studying analgesic drugs. *J. Am. Med. Assoc.* **1955**, *159*, 1619–1622. [CrossRef]
7. Kozak, A.; Marek, P.H.; Pindelska, E. Structural Characterization and Pharmaceutical Properties of Three Novel Cocrystals of Ethenzamide With Aliphatic Dicarboxylic Acids. *J. Pharm. Sci.* **2019**, *108*, 1476–1485. [CrossRef]
8. Surov, A.O.; Manin, A.N.; Voronin, A.P.; Churakov, A.V.; Perlovich, G.L.; Vener, M.V. Weak Interactions Cause Packing Polymorphism in Pharmaceutical Two-Component Crystals. the Case Study of the Salicylamide Cocrystal. *Cryst. Growth Des.* **2017**, *17*, 1425–1437. [CrossRef]
9. Ouyang, J.; Zhou, L.; Liu, Z.; Xiao, S.; Huang, X.; Heng, J.Y.Y. Solubility determination and modelling of benzamide in organic solvents at temperatures from 283.15 K and 323.15 K, and ternary phase diagrams of benzamide-benzoic acid cocrystals in ethanol at 298.15 K. *J. Mol. Liq.* **2019**, *286*, 110855. [CrossRef]
10. Przybyłek, M.; Ziółkowska, D.; Mroczńska, K.; Cysewski, P. Propensity of salicylamide and ethenzamide cocrystallization with aromatic carboxylic acids. *Eur. J. Pharm. Sci.* **2016**, *85*, 132–140. [CrossRef]
11. Cysewski, P.; Przybyłek, M.; Ziółkowska, D.; Mroczńska, K. Exploring the cocrystallization potential of urea and benzamide. *J. Mol. Model.* **2016**, *22*, 103. [CrossRef]
12. Przybyłek, M.; Ziółkowska, D.; Kobierski, M.; Mroczńska, K.; Cysewski, P. Utilization of oriented crystal growth for screening of aromatic carboxylic acids cocrystallization with urea. *J. Cryst. Growth* **2016**, *433*, 128–138. [CrossRef]
13. Mujika, J.I.; Matxain, J.M.; Eriksson, L.A.; Lopez, X. Resonance structures of the amide bond: The advantages of planarity. *Chem. A Eur. J.* **2006**, *12*, 7215–7224. [CrossRef] [PubMed]
14. Vallejo Narváez, W.E.; Jiménez, E.I.; Romero-Montalvo, E.; Sauza-De La Vega, A.; Quiroz-García, B.; Hernández-Rodríguez, M.; Rocha-Rinza, T. Acidity and basicity interplay in amide and imide self-association. *Chem. Sci.* **2018**, *9*, 4402–4413. [CrossRef]
15. Molchanov, S.; Gryff-Keller, A. Solvation of Amides in DMSO and CDCl₃: An Attempt at Quantitative DFT-Based Interpretation of ¹H and ¹³C NMR Chemical Shifts. *J. Phys. Chem. A* **2017**, *121*, 9645–9653. [CrossRef] [PubMed]
16. Chand, A.; Chowdhuri, S. Effects of dimethyl sulfoxide on the hydrogen bonding structure and dynamics of aqueous N-methylacetamide solution. *J. Chem. Sci.* **2016**, *128*, 991–1001. [CrossRef]
17. McQuade, D.T.; McKay, S.L.; Powell, D.R.; Gellman, S.H. Indifference to hydrogen bonding in a family of secondary amides. *J. Am. Chem. Soc.* **1997**, *119*, 8528–8532. [CrossRef]
18. Cysewski, P.; Przybyłek, M.; Kowalska, A.; Tymorek, N. Thermodynamics and intermolecular interactions of nicotinamide in neat and binary solutions: Experimental measurements and COSMO-RS concentration dependent reactions investigations. *Int. J. Mol. Sci.* **2021**, *22*, 7365. [CrossRef]
19. Almeida, G.G.; Borges, A.; Cordeiro, J.M.M. On the hydrogen bonding between N-methylformamide and acetone and tetrahydrofuran. *Chem. Phys.* **2014**, *434*, 25–29. [CrossRef]
20. Nain, A.K. Densities and volumetric properties of (acetonitrile + an amide) binary mixtures at temperatures between 293.15 K and 318.15 K. *J. Chem. Thermodyn.* **2006**, *38*, 1362–1370. [CrossRef]
21. Fink, C.; Sun, D.; Wagner, K.; Schneider, M.; Bauer, H.; Dolgos, H.; Mäder, K.; Peters, S.A. Evaluating the Role of Solubility in Oral Absorption of Poorly Water-Soluble Drugs Using Physiologically-Based Pharmacokinetic Modeling. *Clin. Pharmacol. Ther.* **2020**, *107*, 650–661. [CrossRef]
22. Fade, V. Link between drug absorption solubility and permeability measurements in Caco-2 cells. *J. Pharm. Sci.* **1998**, *87*, 1604–1607.
23. Dahan, A.; Miller, J.M. The solubility-permeability interplay and its implications in formulation design and development for poorly soluble drugs. *AAPS J.* **2012**, *14*, 244–251. [CrossRef] [PubMed]
24. Omachi, F.; Kaneko, M.; Iijima, R.; Watanabe, M.; Itagaki, F. Relationship between the effects of food on the pharmacokinetics of oral antineoplastic drugs and their physicochemical properties. *J. Pharm. Health Care Sci.* **2019**, *5*, 26. [CrossRef] [PubMed]
25. Kopach, M.; Leahy, D.; Manley, J. The green chemistry approach to pharma manufacturing. *Innov. Pharm. Technol.* **2012**, *43*, 72–75.

26. Płotka-Wasyłka, J.; Rutkowska, M.; Owczarek, K.; Tobiszewski, M.; Namieśnik, J. Extraction with environmentally friendly solvents. *TrAC Trends Anal. Chem.* **2017**, *91*, 12–25. [[CrossRef](#)]
27. Laboukhi-Khorsani, S.; Daoud, K.; Chemat, S. Efficient Solvent Selection Approach for High Solubility of Active Phytochemicals: Application for the Extraction of an Antimalarial Compound from Medicinal Plants. *ACS Sustain. Chem. Eng.* **2017**, *5*, 4332–4339. [[CrossRef](#)]
28. Pedro, S.N.; Freire, C.S.R.; Silvestre, A.J.D.; Freire, M.G. The role of ionic liquids in the pharmaceutical field: An overview of relevant applications. *Int. J. Mol. Sci.* **2020**, *21*, 8298. [[CrossRef](#)]
29. Egorova, K.S.; Gordeev, E.G.; Ananikov, V.P. Biological Activity of Ionic Liquids and Their Application in Pharmaceutics and Medicine. *Chem. Rev.* **2017**, *117*, 7132–7189. [[CrossRef](#)]
30. Hough, W.L.; Rogers, R.D. Ionic liquids then and now: From solvents to materials to active pharmaceutical ingredients. *Bull. Chem. Soc. Jpn.* **2007**, *80*, 2262–2269. [[CrossRef](#)]
31. Md Moshikur, R.; Chowdhury, M.R.; Moniruzzaman, M.; Goto, M. Biocompatible ionic liquids and their applications in pharmaceutics. *Green Chem.* **2020**, *22*, 8116–8139. [[CrossRef](#)]
32. Resende De Azevedo, J.; Letourneau, J.J.; Espitalier, F.; Ré, M.I. Solubility of a new cardioactive prototype drug in ionic liquids. *J. Chem. Eng. Data* **2014**, *59*, 1766–1773. [[CrossRef](#)]
33. Cysewski, P.; Jeliński, T.; Cymerman, P.; Przybyłek, M. Solvent screening for solubility enhancement of theophylline in neat, binary and ternary NADES solvents: New measurements and ensemble machine learning. *Int. J. Mol. Sci.* **2021**, *22*, 7347. [[CrossRef](#)] [[PubMed](#)]
34. Zhang, X.; Su, J.; Chu, X.; Wang, X. A Green Method of Extracting and Recovering Flavonoids from *Acanthopanax senticosus* Using Deep Eutectic Solvents. *Molecules* **2022**, *27*, 923. [[CrossRef](#)] [[PubMed](#)]
35. Vanda, H.; Dai, Y.; Wilson, E.G.; Verpoorte, R.; Choi, Y.H. Green solvents from ionic liquids and deep eutectic solvents to natural deep eutectic solvents. *Comptes Rendus Chim.* **2018**, *21*, 628–638. [[CrossRef](#)]
36. Hilali, S.; Wils, L.; Chevalley, A.; Clément-Larosière, B.; Boudesocque-Delaye, L. Glycerol-based NADES as green solvents for ultrasound-assisted extraction of phycocyanin from *Arthrospira platensis*—RSM optimization and ANN modelling. *Biomass Convers. Biorefinery* **2022**, 1–14. [[CrossRef](#)]
37. Pavlič, B.; Mrkonjić, Ž.; Teslić, N.; Kljakić, A.C.; Pojić, M.; Mandić, A.; Stupar, A.; Santos, F.; Duarte, A.R.C.; Mišan, A. Natural Deep Eutectic Solvent (NADES) Extraction Improves Polyphenol Yield and Antioxidant Activity of Wild Thyme (*Thymus serpyllum* L.) Extracts. *Molecules* **2022**, *27*, 1508. [[CrossRef](#)]
38. Adaka, I.C.; Uzor, P.F. Cyrene as a green solvent in the pharmaceutical industry. In *Green Sustainable Process for Chemical and Environmental Engineering and Science: Solvents for the Pharmaceutical Industry*; Inamuddin, Boddula, R., Ahamed, M.I., Asiri, A.M., Eds.; 2020; pp. 243–248; ISBN 9780128218853.
39. Muheem, A.; Jahangir, M.A.; Baboota, S.; Ali, J. Recent patents and a market overview on green or bio-based solvents for chromatographic analysis: A review. *Pharm. Pat. Anal.* **2021**, *10*, 227–235. [[CrossRef](#)]
40. Cysewski, P.; Przybyłek, M.; Rozalski, R. Experimental and theoretical screening for green solvents improving sulfamethizole solubility. *Materials* **2021**, *14*, 5915. [[CrossRef](#)]
41. Duereh, A.; Sato, Y.; Smith, R.L.; Inomata, H. Methodology for replacing dipolar aprotic solvents used in API processing with safe hydrogen-bond donor and acceptor solvent-pair mixtures. *Org. Process Res. Dev.* **2017**, *21*, 114–124. [[CrossRef](#)]
42. Derrien, M.; Badr, A.; Gosselin, A.; Desjardins, Y.; Angers, P. Optimization of a green process for the extraction of lutein and chlorophyll from spinach by-products using response surface methodology (RSM). *LWT Food Sci. Technol.* **2017**, *79*, 170–177. [[CrossRef](#)]
43. Chaves, J.O.; de Souza, M.C.; da Silva, L.C.; Lachos-Perez, D.; Torres-Mayanga, P.C.; Machado, A.P.D.F.; Forster-Carneiro, T.; Vázquez-Espinosa, M.; González-de-Peredo, A.V.; Barbero, G.F.; et al. Extraction of Flavonoids From Natural Sources Using Modern Techniques. *Front. Chem.* **2020**, *8*, 507887. [[CrossRef](#)] [[PubMed](#)]
44. Delgado, D.R.; Peña Fernández, M.Á.; Martínez, F. Preferential solvation of some sulfonamides in 1,4-dioxane + water co-solvent mixtures at 298.15 K according to the inverse Kirkwood-Buff integrals method. *Rev. Acad. Colomb. Ciencias Exactas Físicas y Nat.* **2014**, *38*, 104–114. [[CrossRef](#)]
45. Jeliński, T.; Bugalska, N.; Koszucka, K.; Przybyłek, M.; Cysewski, P. Solubility of sulfanilamide in binary solvents containing water: Measurements and prediction using Buchowski-Ksiazczak solubility model. *J. Mol. Liq.* **2020**, *319*, 114342. [[CrossRef](#)]
46. Bustamante, P.; Ochoa, R.; Reillo, A.; Escalera, J.B. Chameleonic Effect of Sulfanilamide and Sulfamethazine in Solvent Mixtures. Solubility Curves with Two Maxima. *Chem. Pharm. Bull.* **1994**, *42*, 1129–1133. [[CrossRef](#)]
47. Przybyłek, M.; Kowalska, A.; Tymorek, N.; Dziaman, T.; Cysewski, P. Thermodynamic characteristics of phenacetin in solid state and saturated solutions in several neat and binary solvents. *Molecules* **2021**, *26*, 4078. [[CrossRef](#)]
48. Bustamante, C.; Bustamante, P. Nonlinear enthalpy-entropy compensation for the solubility of phenacetin in dioxane-water solvent mixtures. *J. Pharm. Sci.* **1996**, *85*, 1109–1111. [[CrossRef](#)]
49. Li, W.; Farajtabar, A.; Xing, R.; Zhu, Y.; Zhao, H. Equilibrium solubility determination, solvent effect and preferential solvation of amoxicillin in aqueous co-solvent mixtures of N,N-dimethylformamide, isopropanol, N-methyl pyrrolidone and ethylene glycol. *J. Chem. Thermodyn.* **2020**, *142*, 106010. [[CrossRef](#)]
50. Cárdenas, Z.J.; Jiménez, D.M.; Almanza, O.A.; Jouyban, A.; Martínez, F.; Acree, W.E. Solubility and Preferential Solvation of Caffeine and Theophylline in {Methanol + Water} Mixtures at 298.15 K. *J. Solut. Chem.* **2017**, *46*, 1605–1624. [[CrossRef](#)]

51. Liu, C.; Dang, L.; Bai, W.; Wang, R.; Wei, H. Solid-liquid equilibrium of theophylline in solvent mixtures. *J. Chem. Eng. Data* **2014**, *59*, 263–268. [[CrossRef](#)]
52. Shi, P.; Ma, Y.; Han, D.; Du, S.; Zhang, T.; Li, Z. Uncovering the solubility behavior of vitamin B6 hydrochloride in three aqueous binary solvents by thermodynamic analysis and molecular dynamic simulation. *J. Mol. Liq.* **2019**, *283*, 584–595. [[CrossRef](#)]
53. Zhou, Y.; Han, D.; Tao, T.; Zhang, S.; Wang, J.; Gong, J.; Wang, Y. Solubility measurement, thermodynamic correlation and molecular simulations of uracil in (alcohol + water) binary solvents at (283.15–318.15) K. *J. Mol. Liq.* **2020**, *318*, 114259. [[CrossRef](#)]
54. Liu, Q.; an, C.; Huang, Q.; Liu, B.; Xu, R.; Kong, S.; Wang, J.; Wang, M.; Liu, N. Solubility determination and prediction for FOX-7 in three binary solvents at different temperatures. *J. Energ. Mater.* **2022**, 1–16. [[CrossRef](#)]
55. Jeliński, T.; Kubsik, M.; Cysewski, P. Application of the Solute–Solvent Intermolecular Interactions as Indicator of Caffeine Solubility in Aqueous Binary Aprotic and Proton Acceptor Solvents: Measurements and Quantum Chemistry Computations. *Materials* **2022**, *15*, 2472. [[CrossRef](#)]
56. Hyttinen, N.; Heshmatnezhad, R.; Elm, J.; Kurtén, T.; Prisle, N.L. Technical note: Estimating aqueous solubilities and activity coefficients of mono- And α,ω -dicarboxylic acids using COSMOtherm. *Atmos. Chem. Phys.* **2020**, *20*, 13131–13143. [[CrossRef](#)]
57. Salmar, S.; Vaalma, M.; Vider, H.; Tenno, T.; Kuznetsov, A.; Järv, J.; Tuulmets, A. Reaction kinetics and solubility in water-organic binary solutions are governed by similar solvation equilibria. *J. Phys. Org. Chem.* **2016**, *29*, 118–126. [[CrossRef](#)]
58. Paluch, A.S.; Parameswaran, S.; Liu, S.; Kolavennu, A.; Mobley, D.L. Predicting the excess solubility of acetanilide, acetaminophen, phenacetin, benzocaine, and caffeine in binary water/ethanol mixtures via molecular simulation. *J. Chem. Phys.* **2015**, *142*, 044508. [[CrossRef](#)] [[PubMed](#)]
59. Chinta, S.; Rengaswamy, R. Machine Learning Derived Quantitative Structure Property Relationship (QSPR) to Predict Drug Solubility in Binary Solvent Systems. *Ind. Eng. Chem. Res.* **2019**, *58*, 3082–3092. [[CrossRef](#)]
60. Cao, Z.; Wang, Z.; Gao, F.; Zhu, L.; Sha, J.; Li, Y.; Li, T.; Ren, B. Thermodynamic analysis and molecular dynamic simulation of the solubility of risperidone (form I) in the pure and binary solvents. *J. Mol. Liq.* **2022**, *359*, 119061. [[CrossRef](#)]
61. Cysewski, P.; Jeliński, T.; Procek, D.; Dratwa, A. Solubility of Sulfanilamide and Sulfacetamide in neat solvents: Measurements and interpretation using theoretical predictive models, first principle approach and artificial neural networks. *Fluid Phase Equilib.* **2021**, *529*, 112883. [[CrossRef](#)]
62. Rahimpour, E.; Acree, W.E.; Jouyban, A. Prediction of sulfonamides' solubilities in the mixed solvents using solvation parameters. *J. Mol. Liq.* **2021**, *339*, 116269. [[CrossRef](#)]
63. Rahimpour, E.; Alvani-Alamdari, S.; Acree, W.E.; Jouyban, A. Drug Solubility Correlation Using the Jouyban–Acree Model: Effects of Concentration Units and Error Criteria. *Molecules* **2022**, *27*, 1998. [[CrossRef](#)] [[PubMed](#)]
64. Rezaei, H.; Rahimpour, E.; Zhao, H.; Martinez, F.; Jouyban, A. Solubility measurement and thermodynamic modeling of caffeine in N-methyl-2-pyrrolidone + isopropanol mixtures at different temperatures. *J. Mol. Liq.* **2021**, *336*, 116519. [[CrossRef](#)]
65. Zhang, C.; Wu, J.; Wang, R.; Ma, E.; Wu, L.; Bai, J.; Wang, J. Study of the toluene absorption capacity and mechanism of ionic liquids using COSMO-RS prediction and experimental verification. *Green Energ. Environ.* **2021**, *6*, 339–349. [[CrossRef](#)]
66. Chu, Y.; He, X. MoDooop: An Automated Computational Approach for COSMO-RS Prediction of Biopolymer Solubilities in Ionic Liquids. *ACS Omega* **2019**, *4*, 2337–2343. [[CrossRef](#)] [[PubMed](#)]
67. Klamt, A. Conductor-like screening model for real solvents: A new approach to the quantitative calculation of solvation phenomena. *J. Phys. Chem.* **1995**, *99*, 2224–2235. [[CrossRef](#)]
68. Putnam, R.; Taylor, R.; Klamt, A.; Eckert, F.; Schiller, M. Prediction of infinite dilution activity coefficients using COSMO-RS. *Ind. Eng. Chem. Res.* **2003**, *42*, 3635–3641. [[CrossRef](#)]
69. Diedenhofen, M.; Eckert, F.; Klamt, A. Prediction of infinite dilution activity coefficients of organic compounds in ionic liquids using COSMO-RS. *J. Chem. Eng. Data* **2003**, *48*, 475–479. [[CrossRef](#)]
70. Fermeiglia, M.; Braiuca, P.; Gardossi, L.; Pricl, S.; Halling, P.J. In silico prediction of medium effects on esterification equilibrium using the COSMO-RS method. *Biotechnol. Prog.* **2006**, *22*, 1146–1152. [[CrossRef](#)]
71. Eckert, F.; Diedenhofen, M.; Klamt, A. Towards a first principles prediction of pKa: COSMO-RS and the cluster-continuum approach. *Mol. Phys.* **2010**, *108*, 229–241. [[CrossRef](#)]
72. Andersson, M.P.; Jensen, J.H.; Stipp, S.L.S. Predicting pKa for proteins using COSMO-RS. *PeerJ.* **2013**, *1*, e198. [[CrossRef](#)]
73. Klamt, A. Solvent-screening and co-crystal screening for drug development with COSMO-RS. *J. Cheminform.* **2012**, *4*, O14. [[CrossRef](#)]
74. Loschen, C.; Klamt, A. Solubility prediction, solvate and cocrystal screening as tools for rational crystal engineering. *J. Pharm. Pharmacol.* **2015**, *67*, 803–811. [[CrossRef](#)] [[PubMed](#)]
75. Chapman, C.J.; Groven, L.J. Evaluation of solvate and co-crystal screening methods for CL-20 containing energetic materials. *J. Energ. Mater.* **2021**, 1–15. [[CrossRef](#)]
76. Przybyłek, M.; Ziółkowska, D.; Mroczyńska, K.; Cysewski, P. Applicability of Phenolic Acids as Effective Enhancers of Cocrystal Solubility of Methylxanthines. *Cryst. Growth Des.* **2017**, *17*, 2186–2193. [[CrossRef](#)]
77. Cysewski, P.; Przybyłek, M. Selection of effective cocrystals former for dissolution rate improvement of active pharmaceutical ingredients based on lipoaffinity index. *Eur. J. Pharm. Sci.* **2017**, *107*, 87–96. [[CrossRef](#)]
78. Abdallah, M.M.; Müller, S.; González de Castilla, A.; Gurikov, P.; Matias, A.A.; Bronze, M.D.R.; Fernández, N. Physicochemical characterization and simulation of the solid–liquid equilibrium phase diagram of terpene-based eutectic solvent systems. *Molecules* **2021**, *26*, 1801. [[CrossRef](#)]

79. Przybyłek, M.; Walczak, P.; Ziółkowska, D.; Grela, I.; Cysewski, P. Studies on the solid–liquid equilibria and intermolecular interactions Urea binary mixtures with Sulfanilamide and Sulfacetamide. *J. Chem. Thermodyn.* **2021**, *153*, 106308. [[CrossRef](#)]
80. Freire, M.G.; Santos, L.M.N.B.F.; Marrucho, I.M.; Coutinho, J.A.P. Evaluation of COSMO-RS for the prediction of LLE and VLE of alcohols + ionic liquids. *Fluid Phase Equilib.* **2007**, *255*, 167–178. [[CrossRef](#)]
81. Song, Z.; Wang, J.; Sundmacher, K. Evaluation of COSMO-RS for solid–liquid equilibria prediction of binary eutectic solvent systems. *Green Energ. Environ.* **2021**, *6*, 371–379. [[CrossRef](#)]
82. Klamt, A. The COSMO and COSMO-RS solvation models. *Wiley Interdiscip. Rev. Comput. Mol. Sci.* **2011**, *1*, 699–709. [[CrossRef](#)]
83. Freire, M.G.; Ventura, S.P.M.; Santos, L.M.N.B.F.; Marrucho, I.M.; Coutinho, J.A.P. Evaluation of COSMO-RS for the prediction of LLE and VLE of water and ionic liquids binary systems. *Fluid Phase Equilib.* **2008**, *268*, 74–84. [[CrossRef](#)]
84. Abranches, D.O.; Larriba, M.; Silva, L.P.; Melle-Franco, M.; Palomar, J.F.; Pinho, S.P.; Coutinho, J.A.P. Using COSMO-RS to design choline chloride pharmaceutical eutectic solvents. *Fluid Phase Equilib.* **2019**, *497*, 71–78. [[CrossRef](#)]
85. Silva, L.P.; Fernandez, L.; Conceição, J.H.F.; Martins, M.A.R.; Sosa, A.; Ortega, J.; Pinho, S.P.; Coutinho, J.A.P. Design and Characterization of Sugar-Based Deep Eutectic Solvents Using Conductor-like Screening Model for Real Solvents. *ACS Sustain. Chem. Eng.* **2018**, *6*, 10724–10734. [[CrossRef](#)]
86. Loschen, C.; Klamt, A. Cocrystal Ternary Phase Diagrams from Density Functional Theory and Solvation Thermodynamics. *Cryst. Growth Des.* **2018**, *18*, 5600–5608. [[CrossRef](#)]
87. Nakaoka, M.; Tran, K.V.B.; Yanase, K.; MacHida, H.; Norinaga, K. Prediction of Phase Behavior of CO₂ Absorbents Using Conductor-like Screening Model for Real Solvents (COSMO-RS): An Approach to Identify Phase Separation Solvents of Amine/Ether/Water Systems upon CO₂ Absorption. *Ind. Eng. Chem. Res.* **2020**, *59*, 19020–19029. [[CrossRef](#)]
88. Qin, Y.; Chen, X.; Wang, L.; Wei, X.; Nong, W.; Wei, X.; Liang, J. Experimental Determination and Computational Prediction of Dehydroabietic Acid Solubility in (–)- α -Pinene + (–)- β -Caryophyllene + P-Cymene System. *Molecules* **2022**, *27*, 1220. [[CrossRef](#)] [[PubMed](#)]
89. Wahab, O.O.; Olasunkanmi, L.O.; Govender, K.K.; Govender, P.P. Prediction of aqueous solubility by treatment of COSMO-RS data with empirical solubility equations: The roles of global orbital cut-off and COSMO solvent radius. *Theor. Chem. Acc.* **2019**, *138*, 80. [[CrossRef](#)]
90. Klamt, A.; Eckert, F.; Hornig, M.; Beck, M.E.; Brger, T. Prediction of aqueous solubility of drugs and pesticides with COSMO-RS. *J. Comput. Chem.* **2002**, *23*, 275–281. [[CrossRef](#)]
91. Guo, Z.; Lue, B.M.; Thomasen, K.; Meyer, A.S.; Xu, X. Predictions of flavonoid solubility in ionic liquids by COSMO-RS: Experimental verification, structural elucidation, and solvation characterization. *Green Chem.* **2007**, *9*, 1362–1373. [[CrossRef](#)]
92. Loschen, C.; Klamt, A. Prediction of solubilities and partition coefficients in polymers using COSMO-RS. *Ind. Eng. Chem. Res.* **2014**, *53*, 11478–11487. [[CrossRef](#)]
93. Cysewski, P. Prediction of ethenzamide solubility in organic solvents by explicit inclusions of intermolecular interactions within the framework of COSMO-RS-DARE. *J. Mol. Liq.* **2019**, *290*, 111163. [[CrossRef](#)]
94. Balchandani, S.; Singh, R. COSMO-RS Analysis of CO₂ Solubility in N-Methyldiethanolamine, Sulfolane, and 1-Butyl-3-methylimidazolium Acetate Activated by 2-Methylpiperazine for Postcombustion Carbon Capture. *ACS Omega* **2021**, *6*, 747–761. [[CrossRef](#)] [[PubMed](#)]
95. Motlagh, S.R.; Harun, R.; Biak, D.R.A.; Hussain, S.A.; Ghani, W.A.W.A.K.; Khezri, R.; Wilfred, C.D.; Elgharbawy, A.A.M. Screening of suitable ionic liquids as green solvents for extraction of eicosapentaenoic acid (EPA) from microalgae biomass using COSMO-RS model. *Molecules* **2019**, *24*, 713. [[CrossRef](#)] [[PubMed](#)]
96. Panayiotou, C. Redefining solubility parameters: The partial solvation parameters. *Phys. Chem. Chem. Phys.* **2012**, *14*, 3882–3908. [[CrossRef](#)] [[PubMed](#)]
97. Hernández-Bravo, R.; Miranda, A.D.; Martínez-Mora, O.; Domínguez, Z.; Martínez-Magadán, J.M.; García-Chávez, R.; Domínguez-Esquivel, J.M. Calculation of the Solubility Parameter by COSMO-RS Methods and Its Influence on Asphaltene-Ionic Liquid Interactions. *Ind. Eng. Chem. Res.* **2017**, *56*, 5107–5115. [[CrossRef](#)]
98. Járvas, G.; Quillet, C.; Dallos, A. Estimation of Hansen solubility parameters using multivariate nonlinear QSPR modeling with COSMO screening charge density moments. *Fluid Phase Equilib.* **2011**, *309*, 8–14. [[CrossRef](#)]
99. Boucher, D.S. Solubility parameters and solvent affinities for polycaprolactone: A comparison of methods. *J. Appl. Polym. Sci.* **2020**, *137*, 48908. [[CrossRef](#)]
100. Spieß, A.C.; Eberhard, W.; Peters, M.; Eckstein, M.F.; Greiner, L.; Büchs, J. Prediction of partition coefficients using COSMO-RS: Solvent screening for maximum conversion in biocatalytic two-phase reaction systems. *Chem. Eng. Proc. Proc. Intensif.* **2008**, *47*, 1034–1041. [[CrossRef](#)]
101. Buggert, M.; Cadena, C.; Mokrushina, L.; Smirnova, I.; Maginn, E.J.; Arlt, W. COSMO-RS calculations of partition coefficients: Different tools for conformational search. *Chem. Eng. Technol.* **2009**, *32*, 977–986. [[CrossRef](#)]
102. Tshepelevitsh, S.; Hernits, K.; Leito, I. Prediction of partition and distribution coefficients in various solvent pairs with COSMO-RS. *J. Comput. Aided. Mol. Des.* **2018**, *32*, 711–722. [[CrossRef](#)]
103. Tong, Y.; Shi, F.; Wang, W.; Li, H.; Zhai, S.; Wang, K.; An, Q. Experimental measurement and thermodynamic modelling of ethenzamide solubility in three binary solvent systems. *J. Chem. Thermodyn.* **2021**, *161*, 106553. [[CrossRef](#)]
104. Nordström, F.L.; Rasmuson, Å.C. Solubility and melting properties of salicylamide. *J. Chem. Eng. Data* **2006**, *51*, 1775–1777. [[CrossRef](#)]

105. Sadeghi, M.; Rasmuson, Å.C. Solubility of Salicylic Acid, Salicylamide, and Fenofibrate in Organic Solvents at Low Temperatures. *J. Chem. Eng. Data* **2020**, *65*, 4855–4861. [[CrossRef](#)]
106. Tong, Y.; Wang, Z.; Yang, E.; Pan, B.; Jiang, J.; Dang, L.; Wei, H. Determination and correlation of solubility and solution thermodynamics of ethenzamide in different pure solvents. *Fluid Phase Equilib.* **2016**, *427*, 549–556. [[CrossRef](#)]
107. Blake-Taylor, B.H.; Deleon, V.H.; Acree, W.E.; Abraham, M.H. Mathematical correlation of salicylamide solubilities in organic solvents with the Abraham solvation parameter model. *Phys. Chem. Liq.* **2007**, *45*, 389–398. [[CrossRef](#)]
108. Wang, K.; Shang, Z.; Zhang, J.; Liu, Y.; Han, J.; Tang, W. Solubility Determination and Thermodynamic Correlation of 2-Ethoxybenzamide in 12 Pure Solvents from 288.15 to 328.15 K. *J. Chem. Eng. Data* **2021**, *66*, 1508–1514. [[CrossRef](#)]
109. Wilkes, J.B.; Manning, J.F. Solubility of Benzamide in m-Xylene. *J. Chem. Eng. Data* **1963**, *8*, 234. [[CrossRef](#)]
110. Johnstone, R.D.L.; Lennie, A.R.; Parker, S.F.; Parsons, S.; Pidcock, E.; Richardson, P.R.; Warren, J.E.; Wood, P.A. High-pressure polymorphism in salicylamide. *CrystEngComm* **2010**, *12*, 1065–1078. [[CrossRef](#)]
111. Imran, S.; Hossain, A.; Mahali, K.; Guin, P.S.; Datta, A.; Roy, S. Solubility and peculiar thermodynamical behaviour of 2-aminobenzoic acid in aqueous binary solvent mixtures at 288.15 to 308.15 K. *J. Mol. Liq.* **2020**, *302*, 112566. [[CrossRef](#)]
112. Shakeel, F.; Haq, N.; Salem-Bekhit, M.M.; Raish, M. Solubility and dissolution thermodynamics of sinapic acid in (DMSO + water) binary solvent mixtures at different temperatures. *J. Mol. Liq.* **2017**, *225*, 833–839. [[CrossRef](#)]
113. Lei, Y.; Xiao, S.; Chen, S.; Zhang, H.; Li, H.; Lu, Y. N,N-dimethylformamide-induced acute hepatic failure: A case report and literature review. *Exp. Ther. Med.* **2017**, *14*, 5659–5663. [[CrossRef](#)] [[PubMed](#)]
114. Ponomarev, I.I.; Blagodatskikh, I.V.; Muranov, A.V.; Volkova, Y.A.; Razorenov, D.Y.; Ponomarev, I.I.; Skupov, K.M. Dimethyl sulfoxide as a green solvent for successful precipitative polyheterocyclization based on nucleophilic aromatic substitution, resulting in high molecular weight PIM-1. *Mendeleev Commun.* **2016**, *26*, 362–364. [[CrossRef](#)]
115. Doolin, A.J.; Charles, R.G.; De Castro, C.S.P.; Rodriguez, R.G.; Péan, E.V.; Patidar, R.; Dunlop, T.; Charbonneau, C.; Watson, T.; Davies, M.L. Sustainable solvent selection for the manufacture of methylammonium lead triiodide (MAPbI₃) perovskite solar cells. *Green Chem.* **2021**, *23*, 2471–2486. [[CrossRef](#)]
116. Xie, W.; Li, T.; Chen, C.; Wu, H.; Liang, S.; Chang, H.; Liu, B.; Drioli, E.; Wang, Q.; Crittenden, J.C. Using the Green Solvent Dimethyl Sulfoxide to Replace Traditional Solvents Partly and Fabricating PVC/PVC- g-PEGMA Blended Ultrafiltration Membranes with High Permeability and Rejection. *Ind. Eng. Chem. Res.* **2019**, *58*, 6413–6423. [[CrossRef](#)]
117. Camp, J.E.; Nyamini, S.B.; Scott, F.J. CyreneTM is a green alternative to DMSO as a solvent for antibacterial drug discovery against ESKAPE pathogens. *RSC Med. Chem.* **2020**, *11*, 111–117. [[CrossRef](#)]
118. Verheijen, M.; Lienhard, M.; Schrooders, Y.; Clayton, O.; Nudischer, R.; Boerno, S.; Timmermann, B.; Selevsek, N.; Schlapbach, R.; Gmuender, H.; et al. DMSO induces drastic changes in human cellular processes and epigenetic landscape in vitro. *Sci. Rep.* **2019**, *9*, 4641. [[CrossRef](#)]
119. Martin, V.; Jadhav, S.; Egelund, P.H.G.; Liffert, R.; Johansson Castro, H.; Krüger, T.; Haselmann, K.F.; Thordal Le Quement, S.; Albericio, F.; Dettner, F.; et al. Harnessing polarity and viscosity to identify green binary solvent mixtures as viable alternatives to DMF in solid-phase peptide synthesis. *Green Chem.* **2021**, *23*, 3295–3311. [[CrossRef](#)]
120. Ferrazzano, L.; Corbisiero, D.; Martelli, G.; Tolomelli, A.; Viola, A.; Ricci, A.; Cabri, W. Green solvent mixtures for solid-phase peptide synthesis: A dimethylformamide-free highly efficient synthesis of pharmaceutical-grade peptides. *ACS Sustain. Chem. Eng.* **2019**, *7*, 12867–12877. [[CrossRef](#)]
121. Kumar, A.; Jad, Y.E.; El-Faham, A.; de la Torre, B.G.; Albericio, F. Green solid-phase peptide synthesis 4. γ -Valerolactone and N-formylmorpholine as green solvents for solid phase peptide synthesis. *Tetrahedron Lett.* **2017**, *58*, 2986–2988. [[CrossRef](#)]
122. Jad, Y.E.; Govender, T.; Kruger, H.G.; El-Faham, A.; De La Torre, B.G.; Albericio, F. Green Solid-Phase Peptide Synthesis (GSPPS) 3. Green Solvents for Fmoc Removal in Peptide Chemistry. *Org. Proc. Res. Dev.* **2017**, *21*, 365–369. [[CrossRef](#)]
123. Wegner, K.; Barnes, D.; Manzor, K.; Jardine, A.; Moran, D. Evaluation of greener solvents for solid-phase peptide synthesis. *Green Chem. Lett. Rev.* **2021**, *14*, 152–163. [[CrossRef](#)]
124. Bryan, M.C.; Dunn, P.J.; Entwistle, D.; Gallou, F.; Koenig, S.G.; Hayler, J.D.; Hickey, M.R.; Hughes, S.; Kopach, M.E.; Moine, G.; et al. Key Green Chemistry research areas from a pharmaceutical manufacturers' perspective revisited. *Green Chem.* **2018**, *20*, 5082–5103. [[CrossRef](#)]
125. Jou, F.Y.; Deshmukh, R.D.; Otto, F.D.; Mather, A.E. Solubility of H₂S, CO₂ and CH₄ in N-formyl morpholine. *J. Chem. Soc. Faraday Trans. Phys. Chem. Condens. Phases* **1989**, *85*, 2675–2682. [[CrossRef](#)]
126. Jou, F.Y.; Schmidt, K.A.G.; Mather, A.E. Solubility of ethane in N-formyl morpholine. *J. Chem. Eng. Data* **2003**, *48*, 224–225. [[CrossRef](#)]
127. Jou, F.Y.; Mather, A.E.; Schmidt, K.A.G. Solubility of propane in N-formyl morpholine. *Can. J. Chem. Eng.* **2020**, *98*, 998–1002. [[CrossRef](#)]
128. Miller, M.B.; Chen, D.L.; Luebke, D.R.; Johnson, J.K.; Enick, R.M. Critical assessment of CO₂ solubility in volatile solvents at 298.15 K. *J. Chem. Eng. Data* **2011**, *56*, 1565–1572. [[CrossRef](#)]
129. Freire, M.G.; Carvalho, P.J.; Santos, L.M.N.B.F.; Gomes, L.R.; Marrucho, I.M.; Coutinho, J.A.P. Solubility of water in fluorocarbons: Experimental and COSMO-RS prediction results. *J. Chem. Thermodyn.* **2010**, *42*, 213–219. [[CrossRef](#)]
130. Reinisch, J.; Klamt, A.; Eckert, F.; Diedenhofen, M. Prediction of the temperature dependence of a polyether-water mixture using COSMOtherm. *Fluid Phase Equilib.* **2011**, *310*, 7–10. [[CrossRef](#)]

131. Vilas-Boas, S.M.; Abranches, D.O.; Crespo, E.A.; Ferreira, O.; Coutinho, J.A.P.; Pinho, S.P. Experimental solubility and density studies on aqueous solutions of quaternary ammonium halides, and thermodynamic modelling for melting enthalpy estimations. *J. Mol. Liq.* **2020**, *300*, 112281. [[CrossRef](#)]
132. Arenas, P.; Suárez, I.; Coto, B. Combination of molecular dynamics simulation, COSMO-RS, and experimental study to understand extraction of naphthenic acid. *Sep. Purif. Technol.* **2022**, *280*, 119810. [[CrossRef](#)]
133. Cysewski, P.; Walczak, P.; Ziółkowska, D.; Grela, I.; Przybyłek, M. Experimental and theoretical studies on the Sulfamethazine-Urea and Sulfamethizole-Urea solid-liquid equilibria. *J. Drug Deliv. Sci. Technol.* **2021**, *61*, 102186. [[CrossRef](#)]
134. Salleh, M.Z.M.; Hadj-Kali, M.K.; Hizaddin, H.F.; Ali Hashim, M. Extraction of nitrogen compounds from model fuel using 1-ethyl-3-methylimidazolium methanesulfonate. *Sep. Purif. Technol.* **2018**, *196*, 61–70. [[CrossRef](#)]
135. Sicaire, A.G.; Abert Vian, M.; Fine, F.; Carré, P.; Tostain, S.; Chemat, F. Experimental approach versus COSMO-RS assisted solvent screening for predicting the solubility of rapeseed oil. *OCL Oilseeds Fats Crop. Lipids* **2015**, *22*, D404.
136. Han, J.; Dai, C.; Yu, G.; Lei, Z. Parameterization of COSMO-RS model for ionic liquids. *Green Energy Environ.* **2018**, *3*, 247–265. [[CrossRef](#)]
137. Jeschke, S.; Johansson, P. Predicting the Solubility of Sulfur: A COSMO-RS-Based Approach to Investigate Electrolytes for Li-S Batteries. *Chem. A Eur. J.* **2017**, *23*, 9130–9136. [[CrossRef](#)] [[PubMed](#)]
138. Prat, D.; Wells, A.; Hayler, J.; Sneddon, H.; McElroy, C.R.; Abou-Shehata, S.; Dunn, P.J. CHEM21 selection guide of classical- and less classical-solvents. *Green Chem.* **2015**, *18*, 288–296. [[CrossRef](#)]
139. Prat, D.; Hayler, J.; Wells, A. A survey of solvent selection guides. *Green Chem.* **2014**, *16*, 4546–4551. [[CrossRef](#)]
140. Byrne, F.P.; Jin, S.; Paggiola, G.; Petchey, T.H.M.; Clark, J.H.; Farmer, T.J.; Hunt, A.J.; Robert McElroy, C.; Sherwood, J. Tools and techniques for solvent selection: Green solvent selection guides. *Sustain. Chem. Proc.* **2016**, *4*, 7. [[CrossRef](#)]
141. Jessop, P.G. Searching for green solvents. *Green Chem.* **2011**, *13*, 1391–1398. [[CrossRef](#)]
142. Welton, T. Solvents and sustainable chemistry. *Proc. R. Soc. A Math. Phys. Eng. Sci.* **2015**, *471*, 1–15. [[CrossRef](#)]
143. Larsen, C.; Lundberg, P.; Tang, S.; Råfols-Ribé, J.; Sandström, A.; Mattias Lindh, E.; Wang, J.; Edman, L. A tool for identifying green solvents for printed electronics. *Nat. Commun.* **2021**, *12*, 4510. [[CrossRef](#)] [[PubMed](#)]
144. Venturi, D.M.; Campana, F.; Marmottini, F.; Costantino, F.; Vaccaro, L. Extensive screening of green solvents for safe and sustainable UiO-66 synthesis. *ACS Sustain. Chem. Eng.* **2020**, *8*, 17154–17164. [[CrossRef](#)]
145. U.S. Environmental Protection Agency. Available online: <https://www.epa.gov/> (accessed on 25 April 2022).
146. Cabezas, H.; Harten, P.F.; Green, M.R. Designing Greener Solvents. *Chem. Eng.* **2000**, *107*, 107–109.
147. Harten, P.; Martin, T.; Gonzalez, M.; Young, D. The software tool to find greener solvent replacements, PARIS III. *Environ. Prog. Sustain. Energy* **2020**, *39*, e13331. [[CrossRef](#)] [[PubMed](#)]
148. Li, M.; Harten, P.F.; Cabezas, H. Experiences in designing solvents for the environment. *Ind. Eng. Chem. Res.* **2002**, *41*, 5867–5877. [[CrossRef](#)]
149. Harten, P.F. Program for Assisting the Replacement of Industrial Solvents (PARIS III). In Proceedings of the 18th Annual Green Chemistry & Engineering Conference, North Bethesda, MD, USA, 17–19 June 2014.
150. Harten, P. Finding greener solvent mixtures to replace those used in manufacturing processes -Paris III. In Proceedings of the 3rd International Congress on Sustainability Science and Engineering, ICOSSE, Cincinnati, OH, USA, 11–15 August 2013; pp. 311–331.
151. Kim, S.; Thiessen, P.A.; Bolton, E.E.; Chen, J.; Fu, G.; Gindulyte, A.; Han, L.; He, J.; He, S.; Shoemaker, B.A.; et al. PubChem substance and compound databases. *Nucl. Acids Res.* **2016**, *44*, D1202–D1213. [[CrossRef](#)] [[PubMed](#)]
152. COSMOtherm. version 21.0.0. Dassault Systèmes; Biovia: San Diego, CA, USA, 2020.
153. TURBOMOLE. version 7.5.1. TURBOMOLE GmbH: Frankfurt, Germany, 2020.
154. Grimme, S.; Antony, J.; Ehrlich, S.; Krieg, H. A consistent and accurate ab initio parametrization of density functional dispersion correction (DFT-D) for the 94 elements H-Pu. *J. Chem. Phys.* **2010**, *132*, 154104. [[CrossRef](#)]
155. Neau, S.H.; Flynn, G.L. Solid and Liquid Heat Capacities of n-Alkyl Para-aminobenzoates Near the Melting Point. *Pharm. Res. An Off. J. Am. Assoc. Pharm. Sci.* **1990**, *7*, 1157–1162.
156. Svärd, M.; Hjorth, T.; Bohlin, M.; Rasmuson, Å.C. Calorimetric Properties and Solubility in Five Pure Organic Solvents of N-Methyl- d -Glucamine (Meglumine). *J. Chem. Eng. Data* **2016**, *61*, 1199–1204. [[CrossRef](#)]
157. Neau, S.H.; Bhandarkar, S.V.; Hellmuth, E.W. Differential molar heat capacities to test ideal solubility estimations. *Pharm. Res.* **1997**, *14*, 601–605. [[CrossRef](#)]
158. Svärd, M.; Ahuja, D.; Rasmuson, Å.C. Calorimetric Determination of Cocrystal Thermodynamic Stability: Sulfamethazine-Salicylic Acid Case Study. *Cryst. Growth Des.* **2020**, *20*, 4243–4251. [[CrossRef](#)]
159. Acree, W.; Chickos, J.S. Phase Transition Enthalpy Measurements of Organic and Organometallic Compounds. Sublimation, Vaporization and Fusion Enthalpies From 1880 to 2015. Part 1. C1-C10. *J. Phys. Chem. Ref. Data* **2016**, *45*, 033101. [[CrossRef](#)]